2002-12

Assessing the performance of omni-directional receivers for passing acoustic detection of vocalizing odontocetes: initial analysis

Garcia, Jorge F.

Monterey, California. Naval Postgraduate School

NAVAL POSTGRADUATE SCHOOL
Monterey, California

THESIS

ASSESSING THE PERFORMANCE OF OMNI-DIRECTIONAL RECEIVERS FOR PASSIVE ACOUSTIC DETECTION OF VOCALIZING ODONTOCETES: INITIAL ANALYSIS

by

Jorge F. Garcia

December 2002

Thesis Advisor:	Ching-Sang Chiu
Second Reader:	Curtis A. Collins

Approved for public release, distribution unlimited

This page intentionally left blank

REPORT DOCUMENTATION PAGE			Form Approved OMB No. 0704-0188
Public reporting burden for this collection of information is estimated to average 1 hour per response, including the time for reviewing instruction, searching existing data sources, gathering and maintaining the data needed, and completing and reviewing the collection of information. Send comments regarding this burden estimate or any other aspect of this collection of information, including suggestions for reducing this burden, to Washington headquarters Services, Directorate for Information Operations and Reports, 1215 Jefferson Davis Highway, Suite 1204, Arlington, VA 22202-4302, and to the Office of Management and Budget, Paperwork Reduction Project (0704-0188) Washington DC 20503.			
1. AGENCY USE ONLY *(Leave blank)*	**2. REPORT DATE** December 2002	**3. REPORT TYPE AND DATES COVERED** Master's Thesis	
4. TITLE AND SUBTITLE: **Assessing the Performance of Omni-Directional Receivers for Passive Acoustic Detection of Vocalizing Odontocetes: Initial Analysis**			**5. FUNDING NUMBERS**
6. AUTHOR(S) **Jorge F. Garcia**			
7. PERFORMING ORGANIZATION NAME(S) AND ADDRESS(ES) Naval Postgraduate School Monterey, CA 93943-5000			**8. PERFORMING ORGANIZATION REPORT NUMBER**
9. SPONSORING / MONITORING AGENCY NAME(S) AND ADDRESS(ES) N/A			**10. SPONSORING / MONITORING AGENCY REPORT NUMBER**
11. SUPPLEMENTARY NOTES The views expressed in this thesis are those of the author and do not reflect the official policy or position of the Department of Defense or the U.S. Government.			
12a. DISTRIBUTION / AVAILABILITY STATEMENT Approved for public release, distribution unlimited			**12b. DISTRIBUTION CODE**

13. ABSTRACT ***(maximum 200 words)***

The purpose of this study was to evaluate the performance of passive, omni-directional receivers as means to detect vocalizing Odontocetes. It was necessary to establish probability of detection as a function of a) signal to noise ratio and b) probability of false alarm. For this purpose, a model of the probability distribution function of the detector output was derived from experimental data. For the experiment a series of short duration digital recordings of selected Odontocete vocalizations were broadcast from a moving platform. The vocalizations were monitored and recorded at an underwater array consisting of three vertically distributed hydrophones. Over a period of three days, several hundred iterations of each signal – with the transmitter at ranges varying from 300 meters to 12000 meters – were recorded. A monitoring hydrophone was used to monitor the signal source level. The raw data was fed to two "detectors" consisting of different data processing routines. The output of each detector was subjected to statistical analysis. Other factors also considered in the analysis were: signal used, range, and wind. A statistical test was employed to systematically find a best fit probability distribution function model of detector output. From this empirical model, detector performance was estimated.

14. SUBJECT TERMS Oceanography, Acoustics, Marine Mammals			**15. NUMBER OF PAGES** 60
			16. PRICE CODE
17. SECURITY CLASSIFICATION OF REPORT Unclassified	**18. SECURITY CLASSIFICATION OF THIS PAGE** Unclassified	**19. SECURITY CLASSIFICATION OF ABSTRACT** Unclassified	**20. LIMITATION OF ABSTRACT** UL

This page intentionally left blank

Approved for public release; distribution is unlimited

ASSESSING THE PERFORMANCE OF OMNI-DIRECTIONAL RECEIVERS FOR PASSIVE ACOUSTIC DETECTION OF VOCALIZING ODONTOCETES: INITIAL ANALYSIS

Jorge F. Garcia
Lieutenant, United States Navy
B.S. United States Naval Academy, 1995

Submitted in partial fulfillment of the
requirements for the degree of

MASTER OF SCIENCE IN PHYSICAL OCEANOGRAPHY

from the

NAVAL POSTGRADUATE SCHOOL
December 2002

Author: Jorge F. Garcia

Approved by: Ching-Sang Chiu
Thesis Advisor

Curtis A. Collins
Second Reader

Mary L. Bateen
Chairperson, Department of Oceanography

This page intentionally left blank

ABSTRACT

The purpose of this study was to evaluate the performance of inexpensive, passive, omni-directional receivers as a means to detect vocalizing Odontocetes using conditional statistics. To evaluate and predict performance, it was necessary to establish probability of detection as a function of a) signal to noise ratio or range at a given source level and b) probability of false alarm. For this purpose, a model of the probability distribution function of the detector output was derived from experimental data. For the experiment a series of short duration digital recordings of selected odontocete vocalizations were broadcast underwater from a moving platform. The vocalizations were monitored and digitally recorded at a stationary underwater array consisting of three vertically distributed hydrophones. Over a period of three days, several hundred iterations of each signal – with the transmitter at ranges varying from 300 meters to 12000 meters – were recorded. A monitoring hydrophone (co-located with the transmitter) was used to monitor the signal source level. The raw data was fed to two "automatic detectors" consisting of different data processing routines developed in MATLAB®. The output of each detector was subjected to statistical analysis. Other factors also considered in the analysis were: signal used, range, and wind (as a proxy indicator of noise generated by surface wave action). A statistical test was employed to systematically find a best fit probability distribution function model of detector output. From this empirical model, detector performance was estimated.

This page intentionally left blank

TABLE OF CONTENTS

This page intentionally left blank

ACKNOWLEDGEMENTS

I take this opportunity to express my gratitude and indebtedness to those, without whose help, this project could not have been. I thank my Thesis Advisor, Professor Ching-Sang Chiu for assistance rendered and expertise offered in all aspects and stages of the project. I thank my Academic Advisor, Dr. Curtis Collins for being patient when I wasn't, and for helping me find the right thesis. I am grateful to Commander Rost Parsons (Ret.) for his flawless execution of a complex experiment at sea. To Messrs. Chris Miller and Anu Kumar, for invaluable advice on the art of coercing the computer to do things it didn't want to: thank you kindly.

I also gratefully acknowledge the cheerful cooperation of the crew of *R/V Point Sur*, and the staff of San Clemente Island Underwater Range.

This page intentionally left blank

I. INTRODUCTION

A. BACKGROUND

The U.S Navy has been using sound in the sea for three quarters of a century. Today, acoustic research continues to improve our ability to navigate safely and to detect and prosecute ever quieter and more distant targets. But more importantly, sound provides an exceptional means with which we may probe into and attain a better understanding of the ocean's structure and variability and with it, a better understanding of climate and of our world.

The effects on marine life of high energy anthropogenic noise is still not well understood (Goold, 1997, and Madsen et al., 1999). It is however, generally accepted that the acoustic intensity of navy systems is such that it probably presents health hazards to at least some marine species when in the vicinity of the source. Marine mammals are of particular concern due to their already small numbers as well as the evolutionary kinship we share. It is also likely that their own dependence on underwater acoustics makes them particularly vulnerable.

It is in the interest of science, and of the U.S. Navy, to avoid injuring whales and dolphins. To this end, the development and implementation of an automated system for the passive-acoustic detection of marine mammals would be of great use.

There are many physiological and behavioral differences between the two cetacean suborders of Mysticete (baleen whales) and Odontocete (toothed whales). Most relevantly, the ranges of frequencies where their respective vocalizations take place are considerably distinct. Consequently the problem of automated acoustic detection must be addressed separately for each sub-order. This thesis concerns itself with the detection of Odontocetes.

B. THESIS OBJECTIVES AND APPROACH

The objective of this thesis was to evaluate the performance of inexpensive, passive, omni-directional receivers as a means to detect vocalizing Odontocetes using conditional statistics.

A seven step approach was used to attain this objective. The seven steps are listed below.

1. Gather Data. An experiment was designed to provide a statistically significant amount of odontocete call realizations via an underwater transmitter located at varying ranges from a stationary receiver. The receiver output was digitally recorded *continuously* throughout the experiment and stored into chronologically catalogued files.

2. Extract data. A combination of automated and manual procedures was employed to isolate and catalogue those portions of the collected recordings which contained useful data (data recorded **during** transmissions).

3. Process data. The isolated and catalogued portions of the recordings were fed through a band-pass filter and two data processing routines here referred to as *detectors*. Each detector exploited different aspects of the relationship between the whale vocalization and the surrounding acoustical environment to produce an output time-series in which (ideally) the peak values correspond with times during which a vocalization was received. These peaks are also referred to as "hits".

4. Quantify individual detector output. Once again a combination of automated and manual procedures was employed to extract the relevant information from each detector's output. This information was catalogued alongside range, time, detector, and wind information.

5. Analyze statistics of detector output. A number of probability distribution curves were compared against each detector output using a statistical test as an objective comparator of curve fitness. One of the distributions was then selected on the basis of this test.

6. Empirically recreate detector output statistics. The selected distribution curve was defined by two parameters. A set of defining parameters were then found (for

each range) that best fit the selected distribution to the various actual data sets. This gave an empirical model of detector output distribution as a function of range.

7. Consider detector performance. Detector performance could now be "measured" via the usual means which consists of integrating the relevant distribution curves (for a given range or input SNR) to obtain the areas corresponding to probability of detection and probability of false alarm.

C. OUTLINE

Six different odontocete vocalizations were polled from various internet / marine mammal acoustics expert sources and prepared for underwater broadcast by normalizing and filtering. A complete broadcast was assembled which contained fifty iterations of each of the six signals as well interspaced synthetic tones to be used as "place markers", useful in the subsequent extraction of the data. For clarity, I will henceforth refer to a single realization of a call as a ***signal***, to the fifty contiguous realizations of a call as an ***ensemble***, and to the six ensembles as a ***broadcast***.

Three hydrophones of the San Clemente Island Underwater Range (SCIUR) were chosen as the primary receivers for the experiment. A G-34 acoustic source was used to broadcast the signals at varying distances from the SCIUR range. The G-34 was deployed onboard *R/V Point Sur*. The data collected by the range's three hydrophones was digitally recorded in three separate channels (one for each hydrophone).

At the computer lab the acoustic data was first merged with position and wind speed data from ship's automated logs in order to find the distance corresponding with each transmission as well as an indication of sea state. This was possible because the ship and the recording station used the same GPS time reference.

The collected data was de-meaned to remove potential bias; and then band-pass filtered. Filtering ensured that the signal fed to the detector came only from that range of frequencies where the G-34 source was known to behave predictably (linearly). Then the data was run through two different detectors. These detectors are MATLAB® routines of array cross-correlation where the collected data is vector-multiplied with a reference

signal or a specific function, and then integrated over time. The two kinds of detectors used are *a matched filter*, and an *energy detector*.

The matched filter compares the data with one of the broadcast Odontocete vocalizations (prior to broadcast). This is the ideal detector when the source signal is exactly known (Urick, 1983). For the energy detector the same time series is first squared and then integrated in time over a time-window specified by a gate function of unit amplitude and length equal to that of the reference signal. This results in "detection" whenever **enough acoustic energy** reaches the receiver, regardless of the signal's structure (so long as the frequencies are within the passed band). The energy detector is the optimal detector when *no* information about the source signal is known (Urick, 1983).

The detectors' performance at various ranges, times and sea states (wind speeds) was then subjected to statistical analysis. This analysis ultimately led to estimates of sonar performance.

II. METHOD

A. EXPERIMENT – GATHERING THE DATA

1. Hardware

This section gives a brief description of the three major pieces of equipment used during the experiment: the transmitter, the receiver, and the monitoring hydrophone.

a. Transmitter

A type G-34 transducer (rented from the Underwater Sound Reference Division of the Naval Undersea Warfare Center) was used for the transmission of all signals. The propagation frequencies of interest – where the majority of odontocete vocalization takes place – are in the 1-10 kHz band (Sjare et al. 1985). But, as shown in **Figure 1**, the G-34 has an advertised frequency range of 200 Hz – 5 kHz.

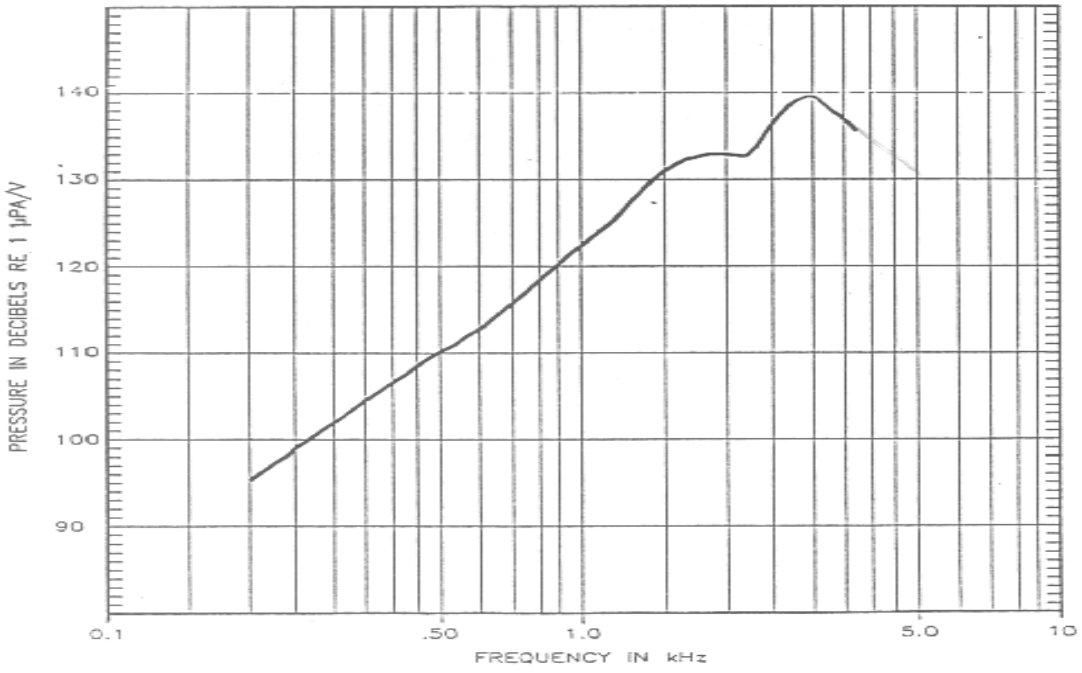

Figure 1: Manufacturer specified Transmit Voltage Response (TVR) curve (Ivey, 1991).

However, an analysis of the data from previous tests with the G34 revealed a slightly larger usable range of up to 8 kHz. By usable it is meant that the frequency dependent response curves extracted from a series of transmissions (100 Hz – 10 kHz up sweeps), remained relatively smooth and stable through this range. As an example, four empirically derived response curves made at different times are shown in **Figure 2**. Note that for frequencies below 8000 Hz, the four curves are overlaid without showing great difference among them. However, above 8000 Hz, a divergence of the curves is clear and it indicates that the source is no longer reliable. The major difference between the manufacturer and the experimental curves is the higher energy at low frequencies for the experimental curves. This is due to background noise.

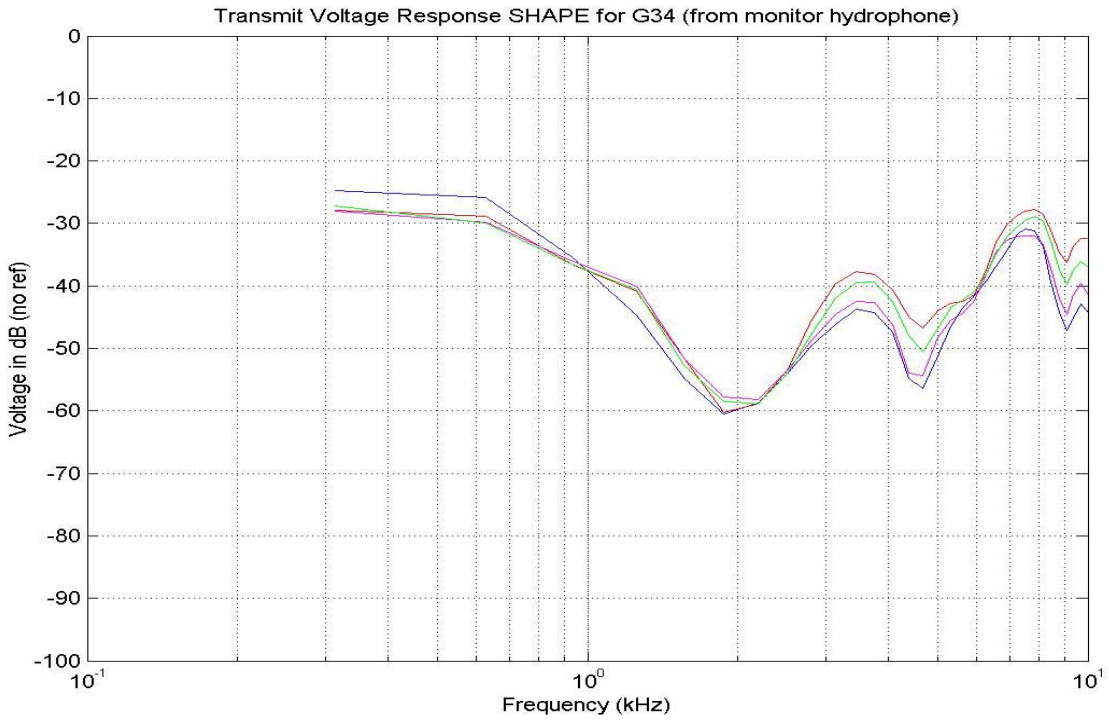

Figure 2: Four experimentally derived transmission voltage response curves correspond to the spectra of four continuous up-sweep transmissions broadcast at different times.

If a response curve is reproducible, it can later be compensated or accounted for in the analysis. This expanded usage was also important because most of the background noise within the band-pass occurs in the lower half, below 5 kHz (Wentz, 1962). By transmitting up to 8 kHz the signal structure can be better exploited.

For efficiency, all signals were filtered prior to transmission to ensure that the transmitted signal energy was contained within this pass band. Signals were filtered in MATLAB® using an 8th order Butterworth filter. A transmission depth of 30 meters was assumed to be a realistic depth where Odontocetes could be expected to vocalize.

The G-34 is powered through the winch cable. Earlier experiments revealed that the voltage output of this winch cable (the input to the G-34) has its own frequency dependent transfer function. It was speculated this effect was due to inductive effects resulting from the cable coiling around the winch. Though interesting, the effect does not negatively influence this experiment since source level was determined as described in section **C.1.**, from a "third party" calibrated hydrophone at a known (estimated) range from the transmitter.

b. Monitoring Hydrophone

A model HTI-96-MIN hydrophone (0-30kHz, Sensitivity: -164.7 dB re 1V/μPa) built by High Tech was deployed from the *R/V Point Sur* during all transmissions. Transmissions were recorded via this monitoring hydrophone at a sample rate of 33333 Hertz. For all deployments, the hydrophone was streamed from the stern of the ship with 30 meters of scope. Gain was set at 10 and sensitivity (manufacturer specified) was -164 dB re 1V/μPA.

c. Receiver

All other acoustic data used in this thesis was collected by the San Clemente Island Undersea Range (SCIUR). The receiver for this experiment was the Naval Undersea Warfare Center's (NUWC) Ship Self-Radiated Noise Measurement (SSRNM) array located on San Clemente Island. The hydrophones in this array are broadband hydrophones built by International Transducer Corporation (Model ITC – 6050 C). They are in a fixed vertical line array (VLA). The array is located at 33 00' 35.1" N, 118 31' 49.8" W. It has three operating hydrophones at depths of 75.29, 136.55, and 165.81 meters.

2. The Whale Calls

The experiment was designed to provide a statistically significant amount of odontocete call realizations to the receiver. The receiver output was digitally recorded *continuously* throughout the experiment and stored into chronologically catalogued files. Later, the relevant data in these files was extracted and analyzed. Some important characteristics of the transmitted data are discussed in this section.

a. Vocalizations

The term "whale call" is here used in a broad sense. There are actually three types of odontocete vocalizations: whistles, clicks, and pulsed sounds. Their significance and their use vary, and are objects of much study and speculation. The only assumption relevant to this thesis as regards the meaning of these vocalizations is that they are a manifestation of some **very common** odontocete pattern of behavior. In other words, the choice of an **acoustical** detector begins with the conditional premise: *given that an odontocete is vocalizing*.

Each signal (or call) used here is approximately one second in duration and is a fragment of a larger sequence of sounds. The structure of this fragment, however, is such that it has a clear beginning and end. It is also generally apparent that the same – or a similar – structure can be found repeatedly throughout the larger sequence.

The calls used were obtained as digital recordings from the sources listed in the list of references. Six calls were selected from among approximately fifty available, based on the quality of the recording as well as the richness of signal content in the desired (1 kHz to 8 kHz) band.

An attempt was made to compile a sample of manageable size (given the time available for the experiment) that was nonetheless adequately representative of the variability found within the repertoire of Odontocetes. Since Orcas and Pilot Whales are among the most acoustically active (and frequently recorded) in the suborder, two signals from each of these were included in the compilation.

The calls used in the experiment were: two Orca (*Orcinus orca*) whistles, two Pilot Whale (*Globicephala macrorhynchus*) whistles, a click train from a Risso's Dolphin (*Grampus grisseus*), and a click train from a Sperm Whale (*Physeter macrocephalus*). Henceforth they will be referred to by the following abbreviated names: **orca1**, **orca2**, **pilo1**, **pilo2**, **risso**, and **sperm**. Of these six signals, only **orca2** and **pilo1** were analyzed due to time constraints.

c. Variability

The usefulness of the detectors, particularly of the matched filter, depends greatly upon the variability to be encountered in real-world odontocete acoustic activity. It is expected this kind of detector will perform poorly when the signals being transmitted are not nearly identical to the reference signal. It is known that at least some species have a vast inventory of available calls. This, however, does not necessarily mean the matched filter is doomed to fail when confronted with real world data.

Reference calls may be found which are both simple and pervasive (examples of such ubiquitous "calls" in human vocalization would be the sounds *Ah, Hey* or *No* which may be found not only in most conversations in English, but also in nearly every other language – yet they remain characteristically human "calls"). If this is the case with Odontocetes, the matched filter may yet prove useful; especially because – unlike the energy detector – the matched filter has the ability to detect a signal even when the signal to noise ratio is poor.

On the other hand, the matched filter's sensitivity to signal structure can be exploited if employed as a means to classify after detection by an energy detector.

d. Transmission

Each broadcast was structured as follows. Each of the six calls (approximately one second long) was repeated fifty times. The individual realizations were separated by a one second period of no transmission. The ensembles of fifty repetitions (approximately one minute long) were themselves separated by a five second

period. This five second period was further divided into one second of no transmission, followed by a 3 kHz tone for three seconds, followed by one second of no transmission.

The entire broadcast of six calls, fifty times each was done while the ship hove-to and idled declutched, and it took approximately fifteen minutes. Once completed, the ship then transited to the next station, and there commenced a new broadcast. The complete set of broadcasts from shortest to longest range (or vice versa) is referred to throughout this work as a *run*.

The first run of the experiment carried the ship out to 10 km (at 1 km intervals) from the SCIUR range. **Figure 3** shows the ship's track for the first run. Based on real-time spectrograms of receiver data during this run it was estimated that the signal was no longer detectable at ranges beyond 7 or 8 km. Consequently the four subsequent runs of the experiment carried the ship no further than that.

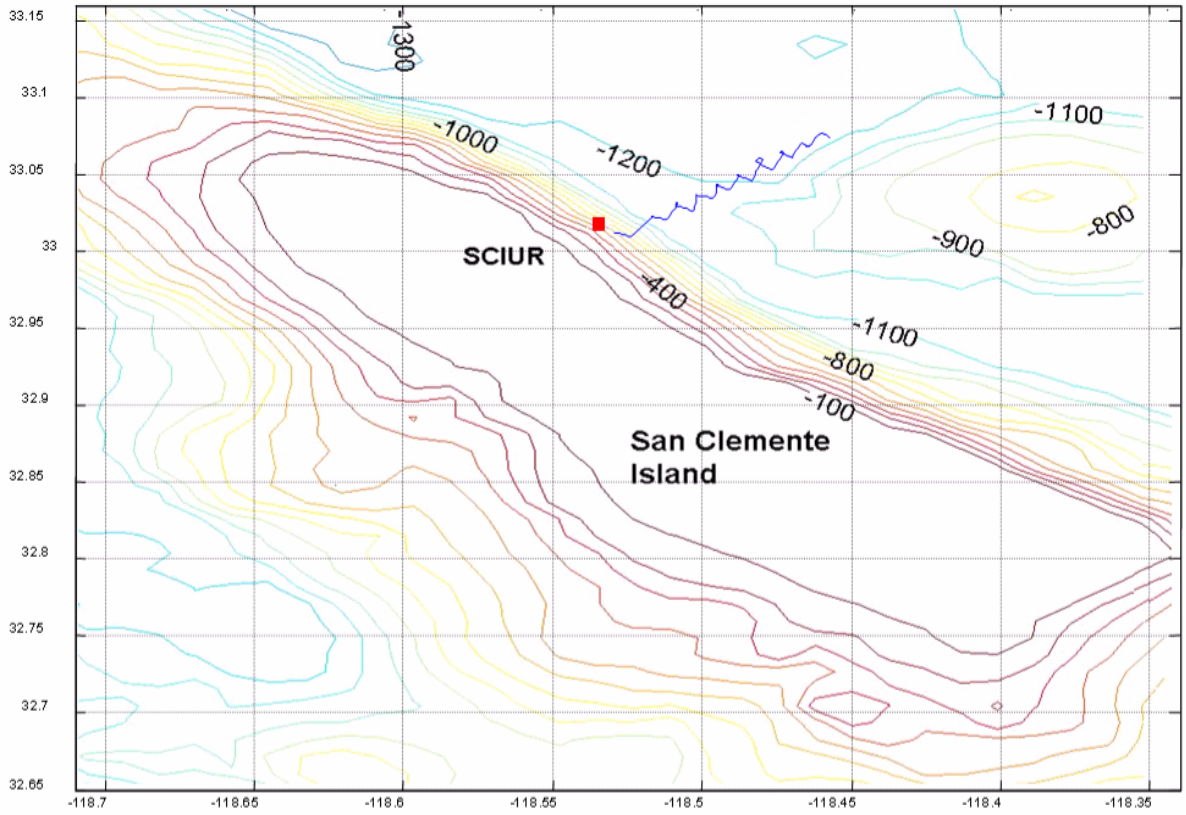

Figure 3: Ship's track for the first run. Receiver array is indicated by red box (■). Note the ship drifted to the southeast while "on station". Chart depths are in meters.

Upon looking at the energy detector output it first became evident that energy from the 3 kHz tone was contaminating the first signal of each ensemble (due to multi-path delayed arrivals). The energy detector showed this first signal as being consistently louder than the other forty-nine. Therefore the MATLAB® routine was made to automatically exclude that first call. For simplicity, however, an ensemble will continue to be referred throughout this work as though it were composed of fifty calls.

For a given voltage, the G-34 produces the highest power output when transmitting at 3 kHz. For this reason, the 3 kHz pulses, marking the start and end of each ensemble, were always easily located in a spectrogram. Once a pulse's location was determined, it could be used as a point of reference. A MATLAB® routine *anchored* on this point of reference then partitioned and extracted the desired ensemble for analysis.

B. EXTRACTING THE DATA

At the SCIUR range, data was recorded almost without interruption for three days. In order to find the desired information within the vast amounts of collected data, the broadcast time (as logged by personnel on watch) was used to provide a coarse idea of where to begin the search. Next, a series of spectrograms were generated for the time series corresponding to the vicinity of this logged time. Within these spectrograms a specific point was located: the leading edge of the second 3 kHz tone. The name of the file containing this point and the sequential location of the point within the file were then integrated into rows in a *locator matrix*.

From this point onward, since the size of each ensemble is exactly known, the process of pulling the desired data could be automated. All later MATLAB® routines made reference to the locator matrix to first locate *the point*. The routines then used incorporated "knowledge" of where the sought data rested relative to *the point*.

Figure 4 shows a "map" of the relative sizes and locations of the first three assemblies in each transmission. This map was used to implement the automated extraction of data. Note how the starting points of several assemblies can be found once a reference point is established. The reference point chosen in this case was CWO2: the leading edge of the 3 kHz tone which marks the start of orca2 (the second 3 kHz tone on

each broadcast). In this example, CWO2 is found within the file daqX+2. The size of each file is exactly known: 2000000 data points (2M), as are the lengths of each of the assemblies. Therefore CWO1 and CWP1 are also known and can be determined by the relationship

$$CWO1 = (4M+CWO1) - ORCA1$$

$$CWP1 = (CWO2+ORCA2) - 4M$$

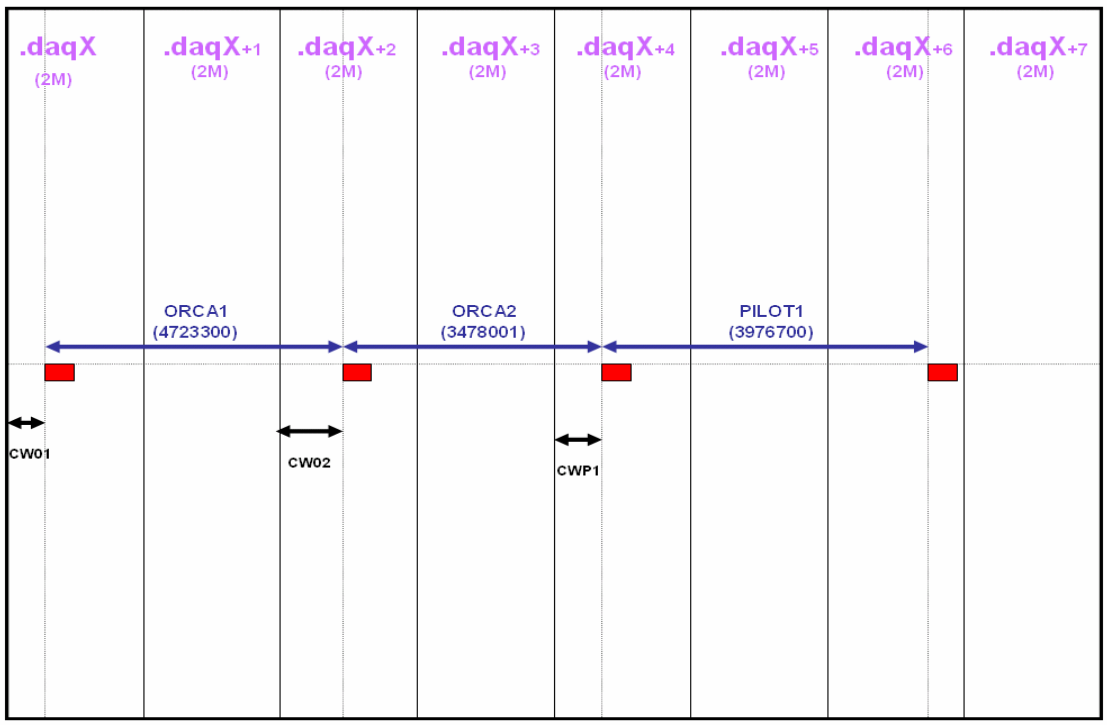

Figure 4: A Map of the first half of the transmission. The red rectangles represent the 3 kHz tones. The vertical black lines show the successive files (.daqX, .daqX+1 …). The numbers in parentheses are the sizes (number of data points) of the corresponding files or signals.

Although automated, the process described was nevertheless time-consuming due to the vast amount of data (a considerably high sample rate of 33333 Hz) being loaded each time. A practical limit of three daq files was incorporated into the routine to bring up the speed of the data analysis process to a tolerable level. The entire ensemble then had to be contained within three files or the routine would not *find* it. Note that due to the length of **orca1** (it exceeds 4M) it necessarily often spanned more than three files. Consequently, a smaller amount of useful data was available from **orca1.** This doesn't mean the data is not there, but that it was – for practical reasons – overlooked.

The starting time of each ensemble was established based on the starting (trigger) time of the daq-file, and the location of the ensemble within this file. This time was then matched with the corresponding time on the ship's log (SAIL data). In this manner, corresponding ship's position and average wind speed information were merged with the data extracted from each ensemble. Since the transmission of an entire ensemble only lasted approximately two minutes – during which the ship hove to while de-clutched – it can be assumed that the position and wind corresponding to its start remained valid for the duration of the transmission. A table containing position and wind information for each extracted ensemble is found in **Appendix A**.

C. PROCESSING THE DATA

Once extracted, the data was processed. The processing had three main objectives: a) to determine the source level (SL) of the calls, b) to filter and correlate the data to produce detector output, and c) to calculate input signal to noise ratio at the receivers.

1. Source Level

Source level (SL) of two different whale calls was established using the method described in the following paragraphs.

a. Finding Range

With the exception of logging cable lengths, no method was devised – during the experiment – to determine with precision the location of either the G-34 or the monitoring hydrophone (nor their relative positions). Consequently the following assumptions were made:

1) The G-34, due to its heavy weight, hung vertically – or nearly so – below the winch.

2) The monitoring hydrophone was located somewhere between hanging directly below its deployment point (at the stern rail of the Point Sur), and streaming directly aft of the Point Sur (near the surface). As shown in **Figure 5** two boundary ranges can be established. If a theoretical source level is calculated for both ranges (and if all other assumptions are correct) then actual source level will necessarily be found somewhere between the two values obtained.

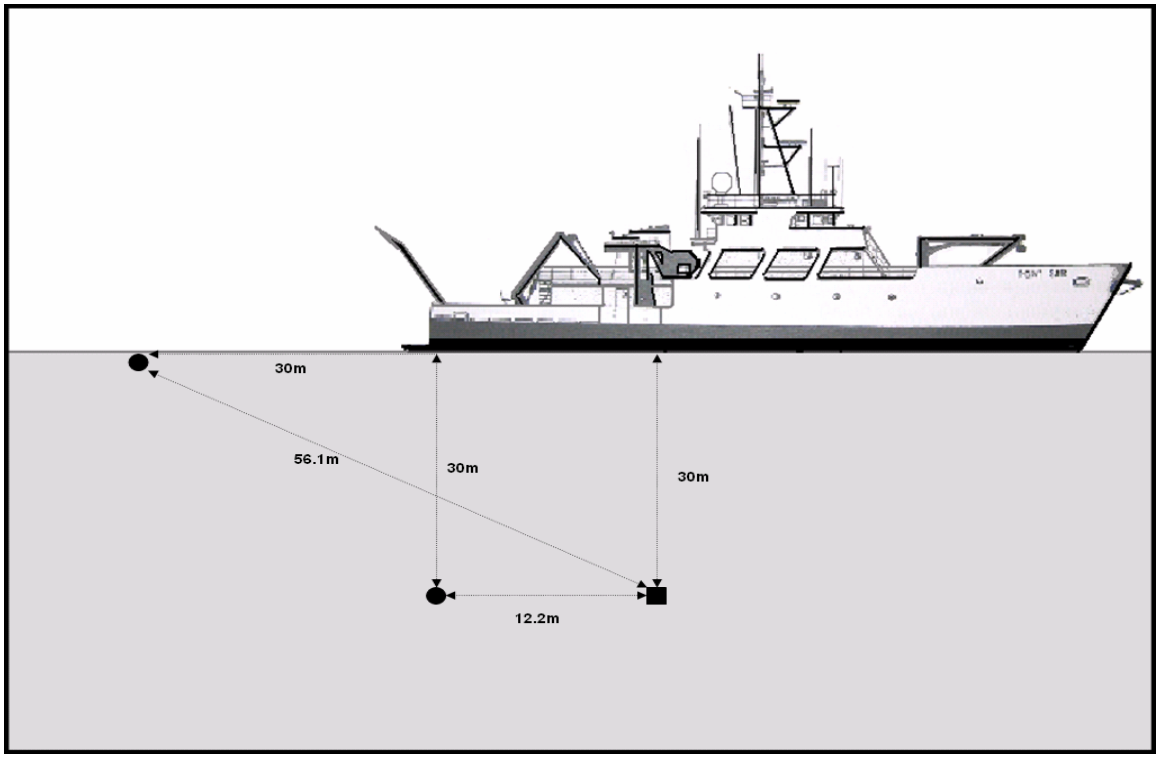

Figure 5: Relative positioning of G-34 source (■) and Monitor Hydrophone (●): maximum (56.1 m) and minimum (12.2 m) ranges.

b. Gain and Sensitivity

The equipment setup for SL monitoring is shown in **Figure 6**. Note that the digitally recorded data – before any manipulation or processing has been applied – has units of volts.

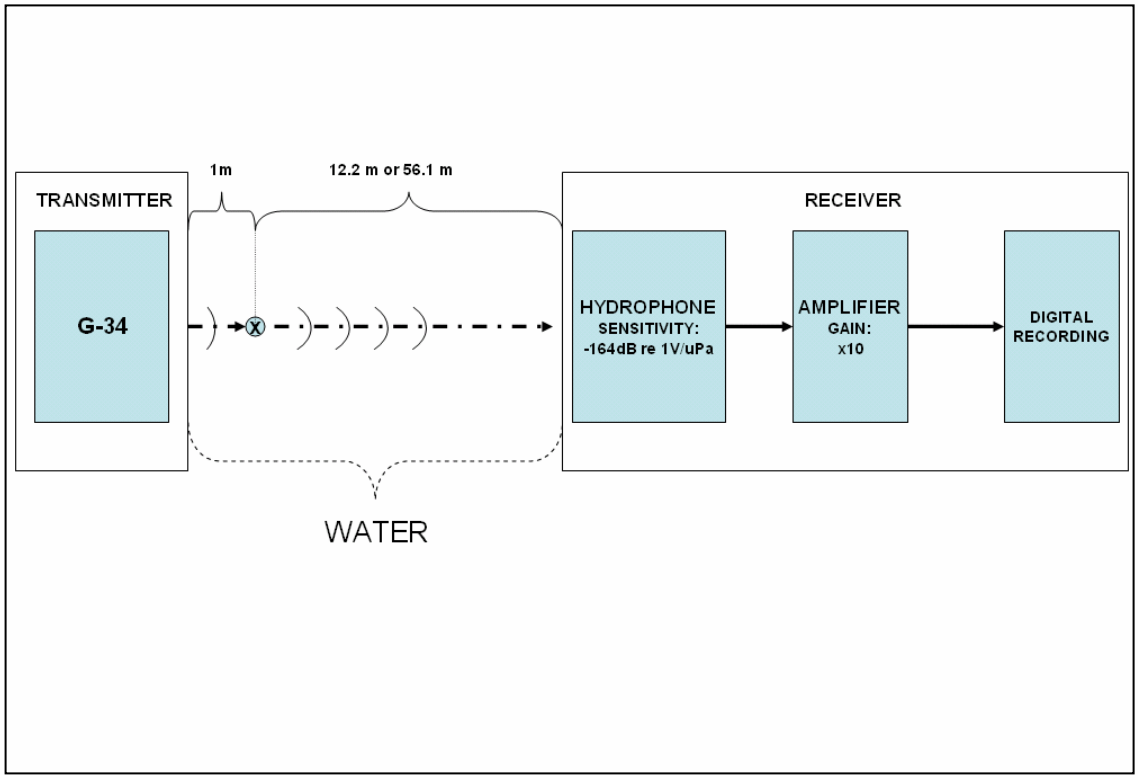

Figure 6: Box diagram of equipment setup for SL estimates. SL is expressed in units of dB re 1 μPa @ 1m. To obtain these units from the data (digital recording) amplifier gain, hydrophone sensitivity and range extrapolation must all be taken into account. Note that the extrapolation is carried to a position 1m from source (marked x) not to the source itself.

Dividing the data by the amplifier gain (volts **upstream** of the amplifier) and then by hydrophone sensitivity returned sound pressure in micro Pascals. This pressure corresponds to a measurement in the water, exactly at the receiver's location. Both gain (setting) and sensitivity (manufacturer specified) were logged for each transmission. They were constant at 10, and -164 dB re 1V/μPA, respectively. Note that since the sensitivity is given in **dB re 1V/μPA**, it needs to be converted to linear scale before the division.

$$Sensitivity_{linear} = 10^{\frac{-164.8}{20}}$$

c. Extrapolation to 1 meter

For Source level estimates, the value of interest is the pressure at a point **1 meter distant from the source**. In spherical spreading the intensity decreases as the square of the range, and the pressure therefore decreases linearly with range. For near distances where the direct path dominates, spherical spreading can be assumed (Urick, 1983). Therefore

$$\mathbf{P_s(t) = D\ P_r(t)}$$

where $\mathbf{P_s(t)}$ is the pressure one meter from the source, **D** is the distance separating the source from monitoring hydrophone, and $\mathbf{P_r(t)}$ is the pressure exactly at the receiver's location.

d. Calculating Source Level

The Data time-series, originally in terms of volts at the receiver has now been manipulated to show micro-Pascals one meter from the source. It remains only to solve for source level. Source level is defined as

$$SL = 10\log_{10}\left(\frac{\frac{1}{T}\int p_0^{\ 2}(t)dt}{1\mu Pa^2}\right)$$

where **T** is the duration of the signal. Individual calls were cropped and isolated out from the relevant time-series to form the time series $\mathbf{P_o^2(t)}$.

e. Results

The two SL values for each call are listed in **Table 1**. Again, recall that if all other assumptions are correct, the actual value of SL for the given signal is found somewhere between the two *boundary* values.

	Orca2	Pilo1
Assuming 12.2 m separation	**141.08** dB re 1μPa@1m	**142.20** dB re 1μPa@1m
Assuming 51.6m separation	**144.81** dB re 1μPa@1m	**145.92** dB re 1μPa@1m

Table 1: SL calculations for orca2 and pilo1

2. Matched Filter

A matched filter is a coherent detector. That means its performance is highly dependent upon the similarity between the signals being compared. It takes advantage of two facts. First, signal and noise are not correlated. Second, the matched filter exploits – in addition to the signal's energy content – the characteristics of the signal waveform.

The matched filter performs the following operation

$$C(m) = \sum_{n=1}^{N} W(m+n)R^*(n)\Delta t$$

where **R** is the reference digital signal, **W** is the digitized received data, **T** (= NΔt) is the integration time, **Δt** is the sampling time interval, and **C** is the detector output (Units of Volts^{2}Seconds). The above equation is implemented in MATLAB® by the function XCORR.

W is the time series spanning one ensemble. In order to asses the performance of the detector, **C** is partitioned into fifty windows and the maximum value within each window is extracted and made part of a fifty element **X** vector (See **Figure 10**).

Note that signal length **T** isn't the same for **orca1, orca2** or **pilo1.** Therefore all reference signals must be normalized the same way if we are to meaningfully compare the detector output using different reference signals. For convenience, each reference signal is normalized to have unit energy. Given a broadcast signal B, of length N, the normalization is

$$R(n) = \frac{B(n)}{\sqrt{\sum_{m=1}^{N} B^2(m)\Delta t}}$$

3. Energy Detector

An energy detector is an incoherent detector: it remains unaffected by spatial or temporal structure of the signal. The energy detector exploits the following aspects of the signal: its energy content, the fact that signal and noise are uncorrelated, and the incoherence of noise. The energy detector performs the following operation

$$C(m) = \sum_{n=1}^{N} W^2(m+n)U(n)\Delta t$$

where U(n) describes a box function duration $\mathbf{N\Delta t}$ with unit amplitude**.**

The detector is insensitive to the actual characteristics of the signal waveform. This presents both an advantage and a disadvantage over the matched filter. The advantage is that its low sensitivity to waveform characteristics results in a less discriminating detector. If classification of the source is not an objective, low discrimination is desirable. The main disadvantage of the energy detector is that it has a much lower *processing gain* (Urick, 1983) than the matched filter and is therefore less likely to detect a signal whose intensity has fallen to the level of background noise.

4. Input Signal to Noise Ratio (SNR) Estimates

Throughout this thesis various references are made to the input signal to noise ratio measured for a given ensemble time-series. The word *input* points to the fact that this is a ratio of signal energy to noise energy at the receiver's location **before** any signal processing takes place. The measurement of input SNR is derived from the energy detector output. Recall that the energy detector integrates the time-series of pressure squared (proportional to power) over a sliding time window. Therefore when the time window position corresponds with a signal in the time-series the corresponding C value is equal to the acoustical energy of the received signal ***plus background noise energy***. When the time window position corresponds with a period of no transmission, the corresponding C value is equal to the background noise energy. Therefore by taking the mean of the energy detector output peaks for a given ensemble, and dividing it by the mean of the output minima (which closely approximates noise energy, i.e. the values

between adjacent peaks) a value **SNNR** is obtained which approximates the ***Signal plus Noise to Noise Ratio***. From this value, an estimated SNR can be obtained as follows

$$\mathbf{SNR_{(linear\ scale)}=SNNR_{(linear\ scale)} - 1}$$

As SNNR approaches 1, SNR (linear scale) approaches zero. But as SNR approaches zero, it is increasingly less likely that the assumption that a peak corresponds with a hit still holds true.

Figure 7 shows how a range-dependent SNR "function" was obtained by interpolation from the collection of estimates. The values shown in Figure 7 are also summarized in **Table 2**.

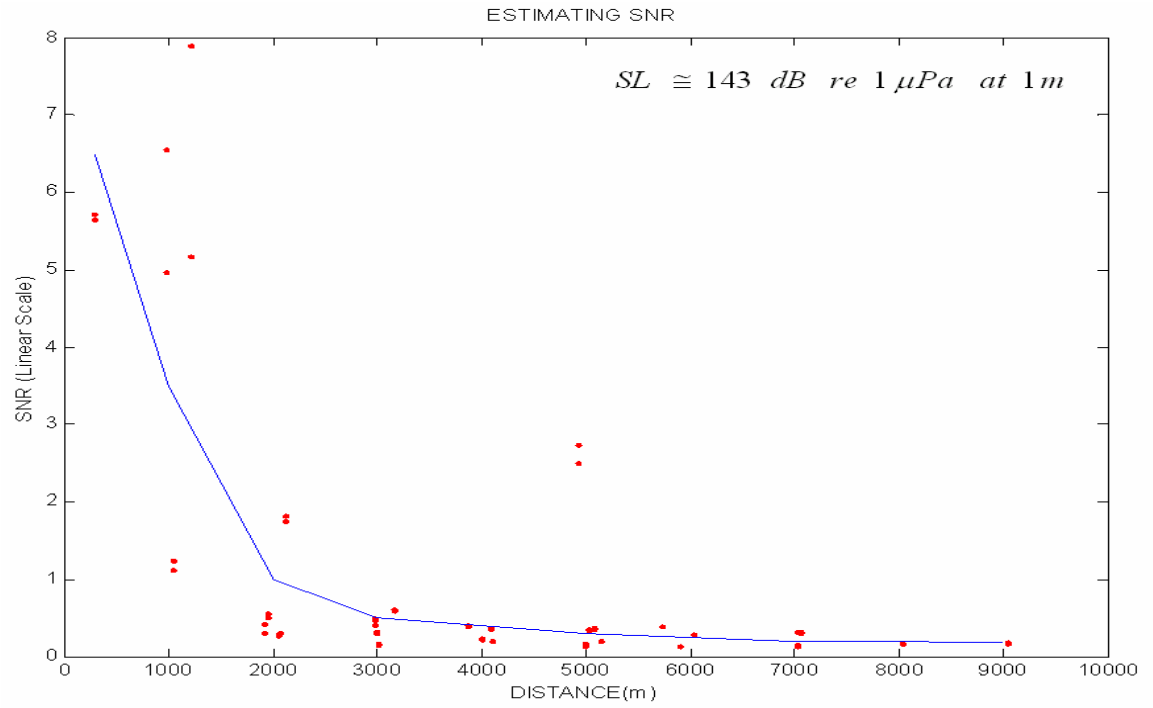

Figure 7: An estimate of input SNR as a function of range estimated from the individual values obtained from the energy detector output.

Range (m)	300	1000	2000	3000	4000	5000	6000	7000	8000	9000
SNR (linear scale)	6.5	3.5	1.0	0.5	0.4	0.3	0.25	0.20	0.19	0.18

Table 2: SNR as a function of range

This page intentionally left blank

III. ANALYSIS AND RESULTS

A. DETECTOR OUTPUT PDF

The primary goal of this thesis was to assess the performance of an omni directional receiver in detecting odontocete vocalizations using statistical measures. With the detector output, this was accomplished using the methods outlined in the following paragraphs.

1. Quantifying Individual Detector Output

Given that the band passed data vector (W) being fed to the detectors spans the period over which an ensemble (50 calls) was transmitted (and received), the output time-series (C) then must contain fifty hits. A *hit* is a peak in the cross-correlation of the reference call (or box-function) with a part of the received time-series which contains exactly one of the transmitted calls. **Figure 8** presents a simplified diagram summary of the MATLAB® implementation of the matched filter. **Figure 9** graphically summarizes the implementation of the energy detector. The two figures highlight the key differences between the detectors as well as show what typical outputs looked like in the presence of a clear (high input SNR) signal. The output of both detectors is given in units of volts squared seconds. In order to obtain units of energy this output needs to be multiplied by the sampling time interval Δt.

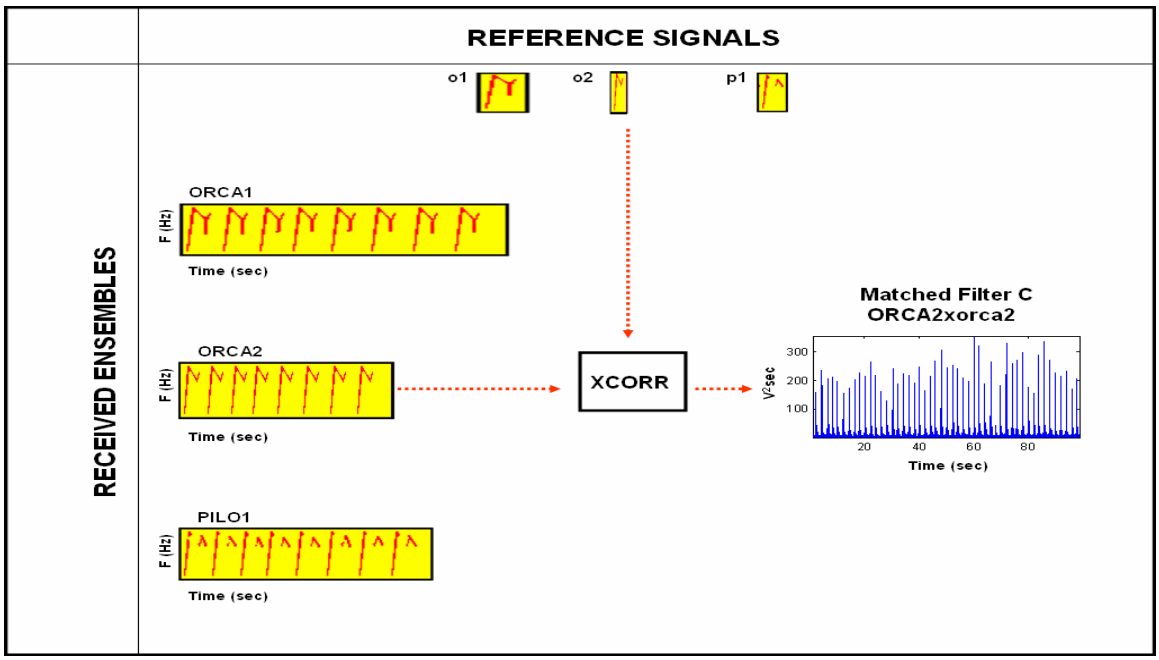

Figure 8: Matched filter. On the left the possible inputs (W) to the detector are represented as simplified spectrograms. These spectrograms each "show" the input which consists of an ensemble of signals. On the top, a simplified spectrogram shows the possible reference signals (R) used by the detector. A reference signal is chosen which matches the input ensemble. On the right, a typical (clean) detector output shows a hit for each realization of the input ensemble.

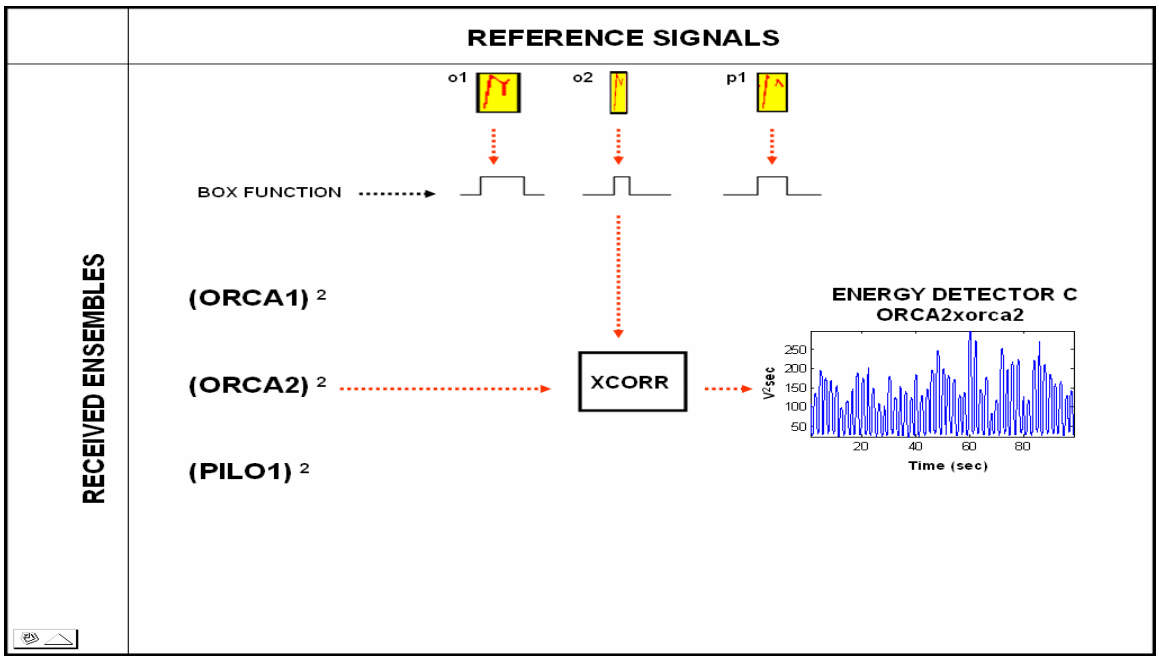

Figure 9: Energy detector. On the left the possible inputs (W^2) to the detector are listed. The diagram shows that the box function is of the same duration as the reference signal (R). On the right, a typical (clean) detector output shows a hit for each realization of the input ensemble.

In order to extract the desired information, the detector output was partitioned into fifty segments (or WINDOWS) of equal length, each of which contained one hit. Recall that the structure of the transmitted ensemble consists of fifty iterations of the reference signal interspaced by one second intervals. This one second interval advantageously insures that the partitioning of the output will not result in an error-inducing amputation of part of the cross-correlated signal.

Figure 10 illustrates the process whereby the detector output peaks for each ensemble are extracted to form a vector of hits **X**. Recall that there are three receiver hydrophones, therefore for any given signal, range, time, detector combination three separate X vectors are produced.

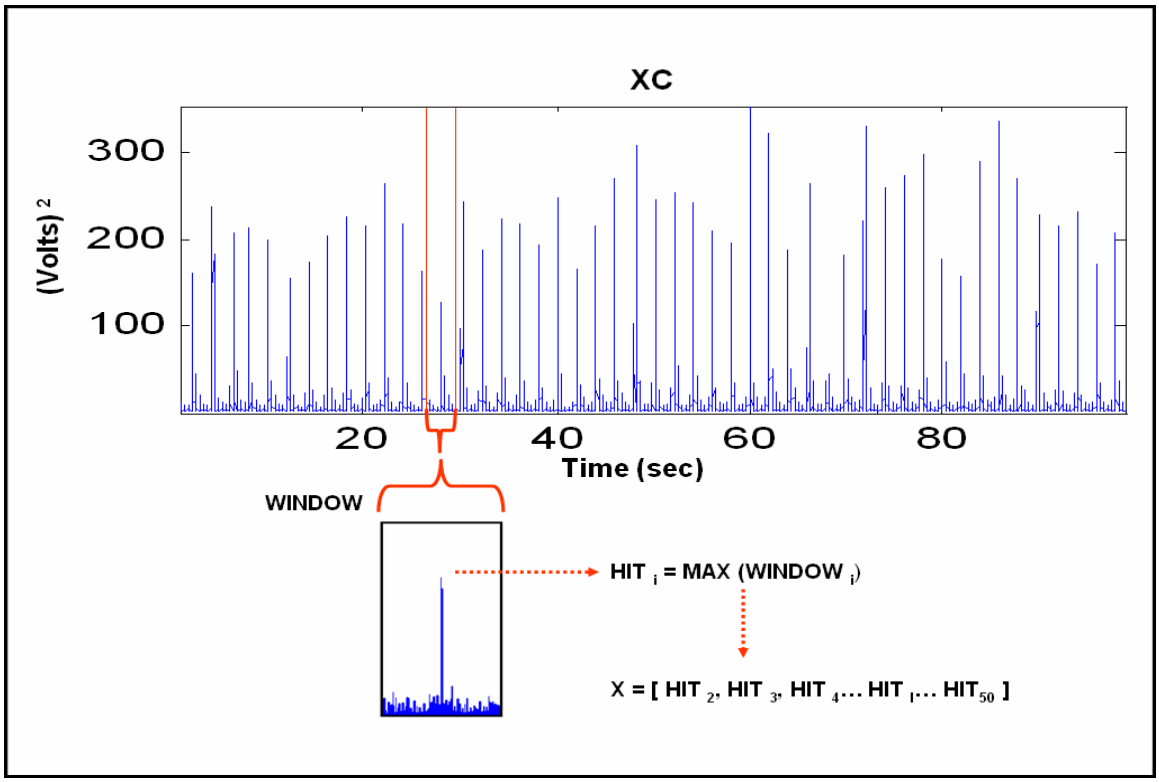

Figure 10: The upper portion of the figure shows the matched filter output given an ensemble input (with adequate SNR). The lower portion of the figure demonstrates the process whereby peak values of the output corresponding with "hits" are extracted to form a fifty element vector X. Once a X vector is produced for each received ensemble, a statistical analysis of detector output peaks can proceed.

The validity of the assumption that peak value in each window corresponds with the value of a "successful" correlation/hit depends upon the input SNR. **Figure 11** illustrates (left side) a case where the value of the hit is lost in the background, and (right side) a case where individual hits still show (barely) above the background. This transition was observed to occur at an SNR of approximately 0.25 (linear scale).

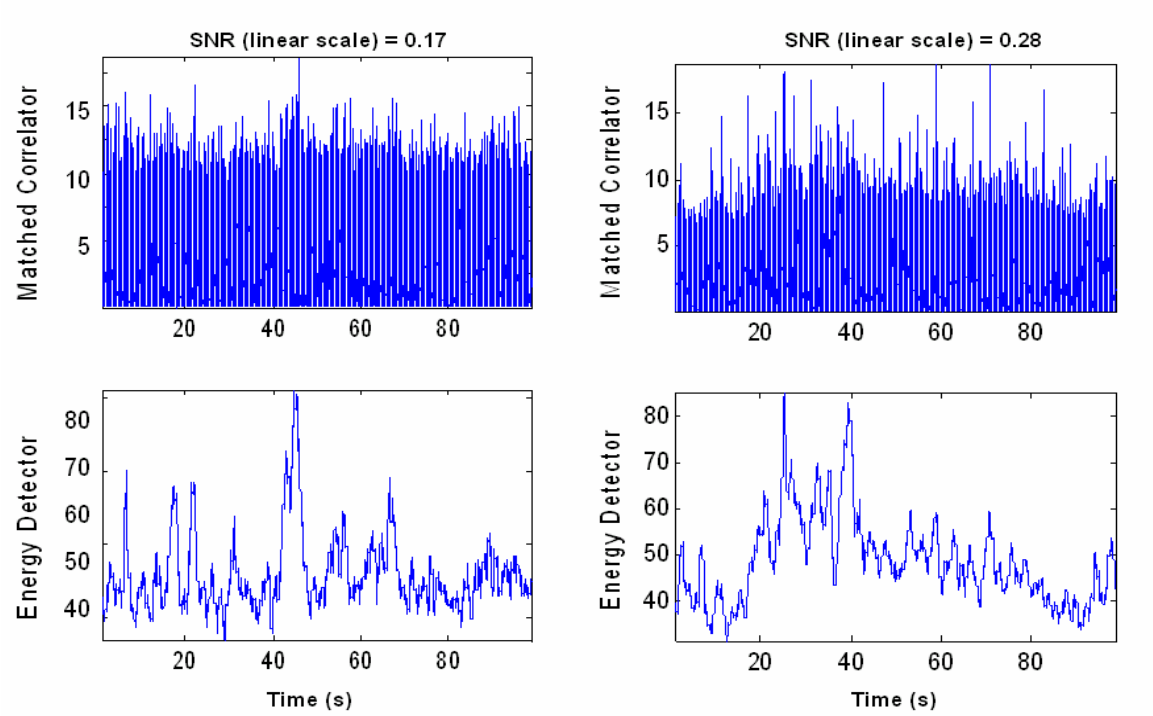

Figure 11: Detector outputs for both detectors with fairly poor input SNR. On the left: Estimated SNR (linear scale) is 0.17 – The individual "hits" are not discernible in either detector's output (Therefore MAX (WINDOW) = HIT) is probably not a valid assumption. On the right: Estimated SNR is 0.28 – The individual "Hits" are still (though barely) discernible. MAX (WINDOW) = HIT, may still be a valid assumption.

2. Analyzing the Statistics of Detector Output

In order to find a best fit continuous probability function (PDF) to describe the statistics of detector hits/peaks, **Normal**, **Gamma**, and **Weibull** distributions were tried. These were chosen because they are the most general forms of their corresponding "families" of distributions. In other words, they were chosen for their flexibility.

The fitness-test performed was a ***Kolmogorov-Smirnov test of the distribution of one sample***. In MATLAB®, KS = **KSTEST** (X, CDF, S) performs the Kolmogorov-

Smirnov test to compare the distribution of X to the hypothesized distribution defined by the two-column matrix CDF. Column one of CDF contains a set of possible x values in X, and column two contains the corresponding hypothesized cumulative distribution function values.

The null hypothesis for the test is that X conforms to the distribution specified by CDF. The alternative hypothesis is that it does not. Therefore, KS = 1 if we can reject the hypothesis that X has a CDF-like distribution. KS = 0 if we can't reject.

S specifies the significance level; or the tolerated probability of incorrectly rejecting the hypothesis. In other words, the probability that for a distribution which **is** CDF-like, and erroneous verdict of KS = 1 will be assigned. S is a useful parameter in that it can be adjusted such that it optimizes the ability of **KSTEST** to **discern** between the relative fitness "competing" distributions. S was fixed at 0.5 for the all tests referred to in this thesis.

The MATLAB® Kolmogorov-Smirnov requires a hypothetical cumulative distribution function as one of the input arguments. It was derived using MATLAB® as follows:

1) P = *DIST* FIT (X) returned the maximum likelihood estimates for the parameters of distribution *DIST* (NORMAL, GAMMA, or WEIBULL) given the data in the vector X. For instance, P = NORMALFIT (X) yields the two parameter vector P, where P (1) is the mean of X, and P(2) is its standard deviation.

2) **Figure 12** shows a "typical" cumulative distribution used in the test. It was obtained by Y = *NORMAL*CDF (X_r, P (1), P (2)), where X_r is an incremental vector which contains the range of X, and P(1) and P(2) were obtained from 1) above.

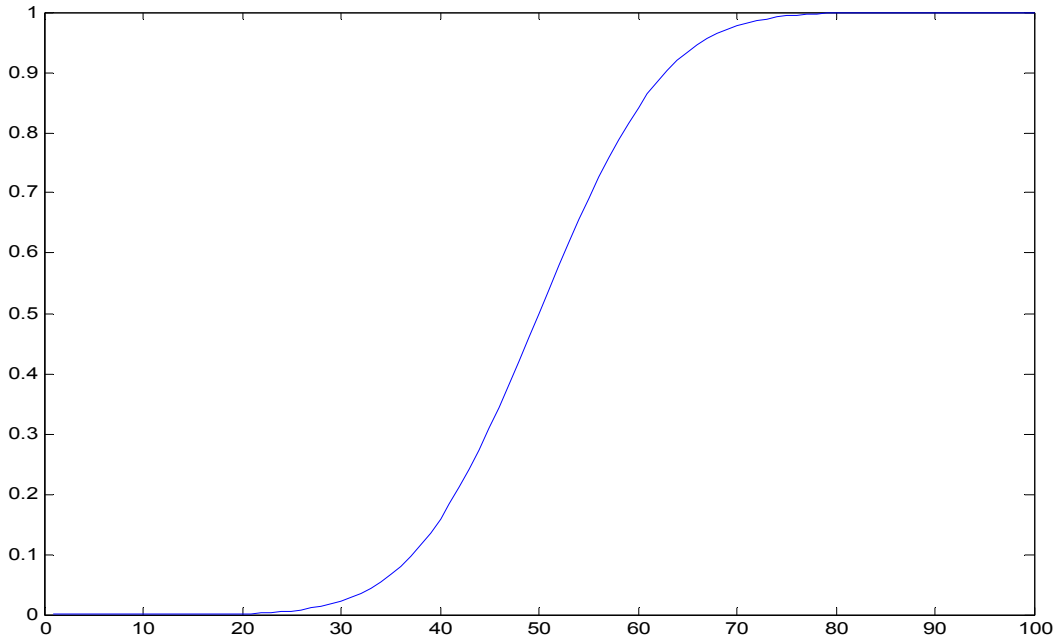

Figure 12: A normal cumulative distribution curve defined by a mean of 50 and a standard deviation of 10 and given an X_r = [1:100]

3) The two column matrix CDF = [X_r, Y] constitutes the second argument – along with X – required by KSTEST (as explained above).

The MATLAB® function PDF *DIST* works like CDF *DIST* but its output is the specified **probability distribution function**. This function was used to generate the curves which were then superimposed on the histograms of corresponding X. Several examples of detector output peak distribution histograms and their corresponding best fit PDF curves are shown in **Figure 13**. These curves were useful because they allowed some measure of visual validation of the Kolmogorov-Smirnov test results.

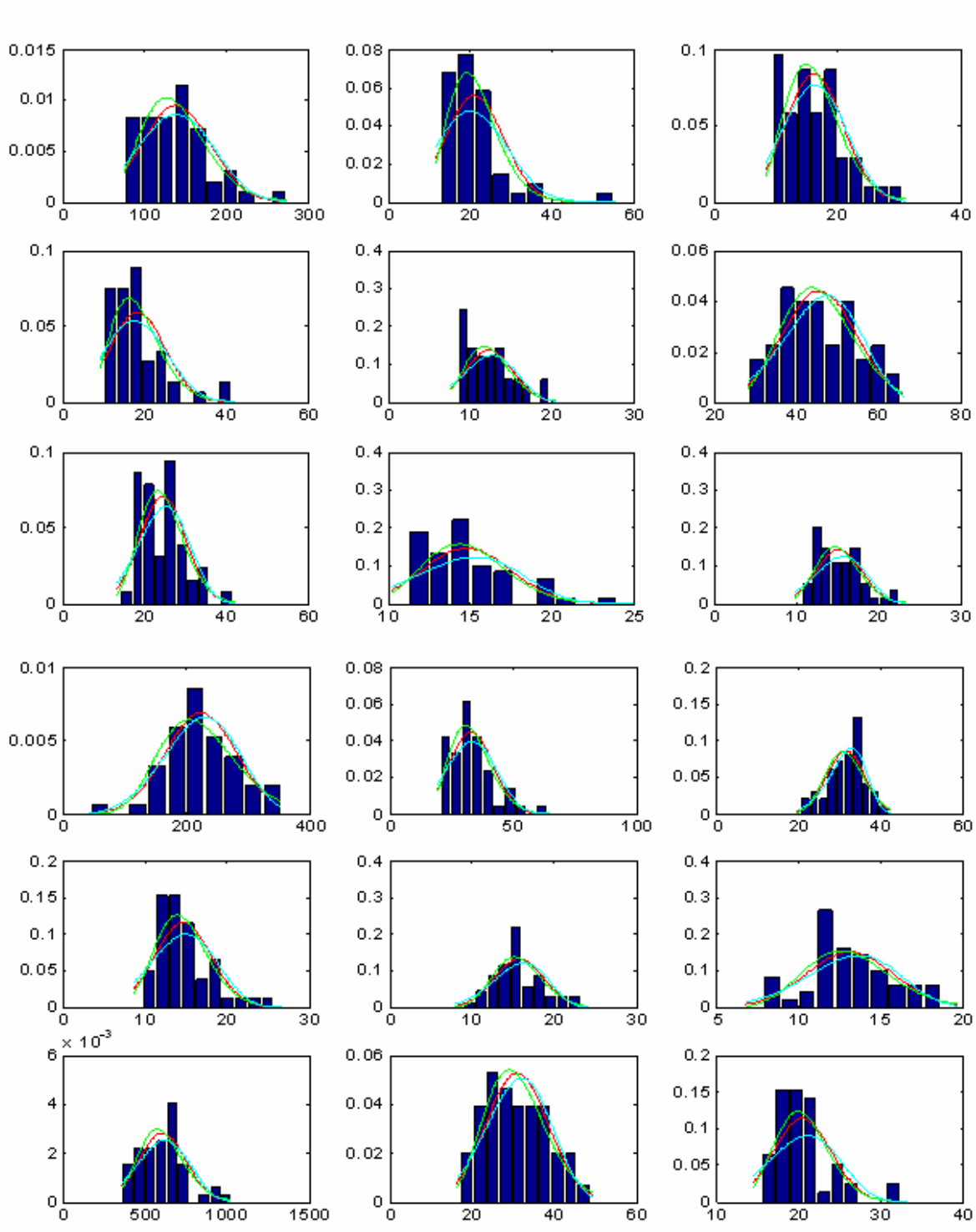

Figure 13: Various samples of fitted probability distribution functions. The distributions tested: Red – Normal, Green – Gamma, and Blue – Weibull. These samples are taken from the matched filter data, channel-three, for ranges between 1000 and 7000 meters. All have estimated input SNR (linear scale) greater than 0.3.

3. Best Fit PDF as a Function of Range

Two hundred and sixty-four X vectors, corresponding to the outputs from both detectors where an **orca2** ensemble was the input, were curve-fit tested. The X vectors were first separated by visual estimate of the corresponding filter output © into high and low SNR in order to contrast detector output statistics in mostly noise conditions with detector statistics in the presence of a clear signal. The results of the tests are shown in **Tables 3 and 4**

CALL	CH	SNR	NORMAL REJECTIONS	GAMMA REJECTIONS	WEIBULL REJECTIONS
O2xo2	2	HIGH	14	12	25
O2xo2	3	HIGH	18	14	25
O1xo1	2	HIGH	0	0	4
O1xo1	3	HIGH	2	2	4
P1xp1	2	HIGH	2	1	4
P1xp1	3	HIGH	3	1	4
SUM			**39**	**30**	**66**
%			**59**	**45**	**100**
O2xo2	2	LOW	3	3	4
O2xo2	3	LOW	3	3	4
O1xo1	2	LOW	3	3	7
O1xo1	3	LOW	6	5	7
P1xp1	2	LOW	5	4	10
P1xp1	3	LOW	7	5	10
SUM			**27**	**23**	**42**
%			**64**	**55**	**100**
Noisexo2	2	N/A	4	3	4
Noisexo2	3	N/A	3	3	4
Noisexo1	2	N/A	3	3	4
Noisexo1	3	N/A	1	1	4
Noisexp1	2	N/A	3	2	4
Noisexp1	3	N/A	1	1	4
SUM			**15**	**13**	**24**
%			**63**	**54**	**100**

Table 3: Number and percent of rejections of "fits" of energy detector PDF to normal, gamma, and Weibull distributions by the Kolmogorov-Smirnov test of the distribution of one sample. The data was grouped into three general types: data with high SNR (upper third of table), data with low SNR (middle third), and pure background noise (bottom third).

CALL	CH	SNR	NORMAL REJECTIONS	GAMMA REJECTIONS	WEIBULL REJECTIONS
O2xo2	2	HIGH	9	7	25
O2xo2	3	HIGH	13	6	25
O1xo1	2	HIGH	2	1	4
O1xo1	3	HIGH	1	1	4
P1xp1	2	HIGH	0	0	4
P1xp1	3	HIGH	1	0	4
SUM			**26**	**15**	**66**
%			**39**	**23**	**100**
O2xo2	2	LOW	2	2	4
O2xo2	3	LOW	1	1	4
O1xo1	2	LOW	3	2	7
O1xo1	3	LOW	4	4	7
P1xp1	2	LOW	6	5	10
P1xp1	3	LOW	5	4	10
SUM			**21**	**18**	**42**
%			**50**	**43**	**100**
Noisexo2	2	N/A	2	1	4
Noisexo2	3	N/A	2	2	4
Noisexo1	2	N/A	3	3	4
Noisexo1	3	N/A	4	3	4
Noisexp1	2	N/A	4	4	4
Noisexp1	3	N/A	4	4	4
SUM			**19**	**13**	**24**
%			**79**	**54**	**100**

Table 4: Number and percent of rejections of "fits" of matched filter PDF to normal, gamma, and Weibull distributions by the Kolmogorov-Smirnov test of the distribution of one sample. The data was grouped into three general types: data with high SNR (upper third of table), data with low SNR (middle third), and pure background noise (bottom third).

The figures in the highlighted rows represent the total number (and percentage) of rejections of the hypothesis that the given distribution (at the top of each column) matched the distribution of X. So for instance, out of 66 high SNR X vectors, the hypothesis that they exhibited a Weibull distribution was rejected 66 times (100% rejection). However, for the same 66 X vectors, the hypothesis that they exhibited a gamma distribution was rejected only 15 times (23% rejection). From a comparison of the various results, it is clear that the best fitting distribution (the one least often rejected) is the gamma distribution. It is furthermore apparent that the gamma distribution is a better fit for detector performance **in the presence** of signal. Also, the matched filter performance is more closely approximated by the gamma distribution than that of the energy detector.

Like the normal, the gamma distribution is a two-parameter curve. It is a non-symmetric curve expressed mathematically as

$$G(x) = \frac{(x/g_1)^{g_2-1} e^{-x/g_1}}{g_1 \Gamma(g_2)}$$

The gamma scale parameter (g_1) and the gamma shape parameter (g_2) are related to the mean $\bar{x}$ and the variance s^2 as follows

$$\hat{g}_1 = \frac{s^2}{\bar{x}} \quad \text{and} \quad \hat{g}_2 = \frac{\bar{x}^2}{s^2}$$

The MATLAB® function GAMMAFIT was used once again to obtain the values of g_1 and g_2 for each range, time, and detector. This time the values were tabulated according to range and then plotted versus range. Using these plots, a representative value for g_1 and g_2 for **each range** could be approximated by interpolation. The individual values and the interpolation are shown on **Figure 14** and **Figure 15** for the matched milter and the energy detector respectively. Parameters g_1 and g_2 were estimated only up to 5000 m for the energy detector and 9000 m for the matched filter.

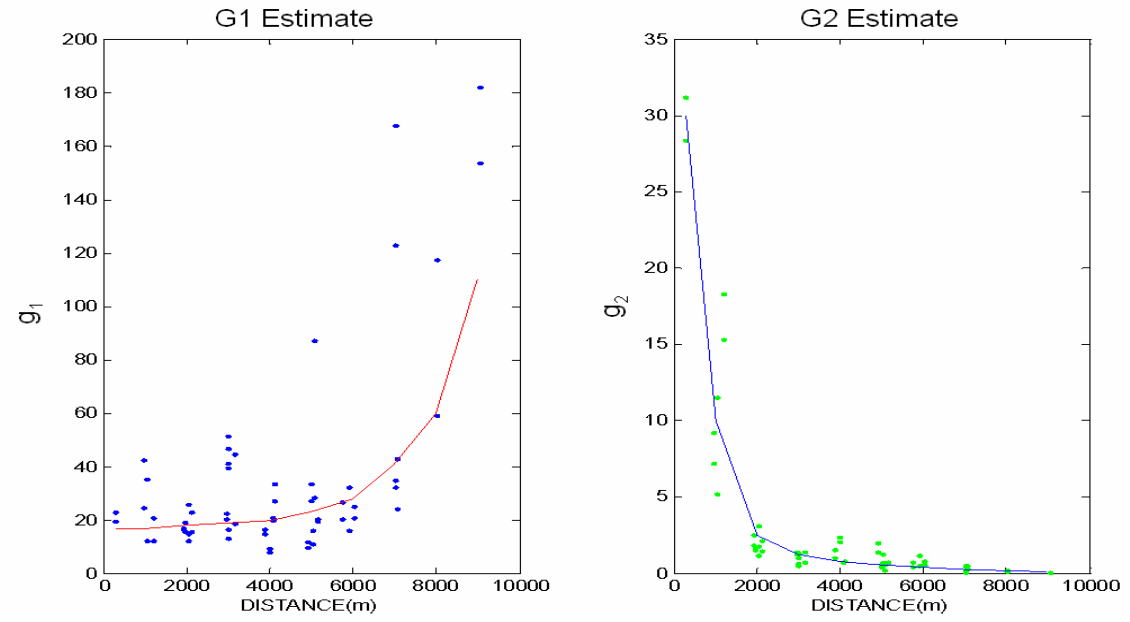

Figure 14: Estimated g1 and g2 values for the matched filter output. The blue/green dots represent the values estimated for each X vector. From these, for each range (300 m, 1000 m, 2000 m, 3000 m, 4000 m, 5000 m, 6000 m, 7000 m, 8000 m, 9000 m) a single value of g1 and g2 was estimated (red/blue line).

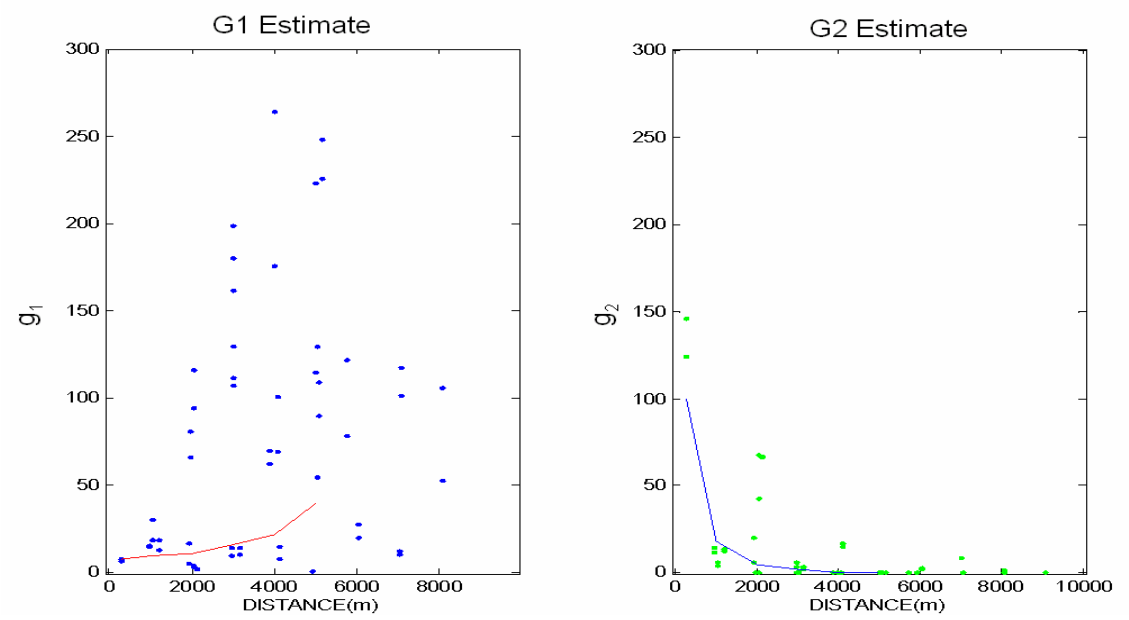

Figure 15: Estimated g1 and g2 values for the energy detector output. The blue/green dots represent the values estimated for each X vector. From these, for each range (300 m, 1000 m, 2000 m, 3000 m, 4000 m, and 5000 m) a single value of g1 and g2 was estimated (red/blue line).

It is evident in **Figure 15** that the g1 parameter value is more scattered for the energy detector suggesting the effects of higher sensitivity of the energy detector to discrete noise which is non-stationary. Consequently the energy detector results must be considered less reliable as those for the matched filter. As will be discussed on a later section, the energy detector is very sensitive to discrete noises to which the matched filter is relative immune. Discrete noises are transient noises, such as those produced by a passing fast boat, or an active navy sonar. In the presence of said discrete noise sources the energy detector invariably produces anomalous g1 values.

The estimated values of g_1 and g_2 used to calculate detector performance measures (shown as solid lines in **Figures 14 and 15**) are listed in **Table 3**. **Figure 16** shows the gamma probability distribution functions that best fit the detector output peaks. Each detector's output distribution is thus described in terms of a continuous curve for each range. These curves provide the basis for discussion and comparison of detector performance.

ENERGY DETECTOR P(D)										
RANGE(m)										
	0300	1000	2000	3000	4000	5000	6000	7000	8000	NOISE
g1	8	10	11	16	22					40
g2	100	18	5	2	0.6					0.2
MATCHED FILTER P(D)										
RANGE(m)										
	0300	1000	2000	3000	4000	5000	6000	7000	8000	NOISE
g1	17	17	18	19	20	23	28	41	60	110
g2	30	10	2.5	1.25	0.75	0.55	0.4	0.25	0.15	0.08

Table 5: Estimated values of g1 and g2 versus range for both detectors. These values were used in the best fit PDF curve. Note that the column labeled "noise" describes the distribution of detector output for ranges greater than 4000 m (energy detector) or 8000 m (matched filter).

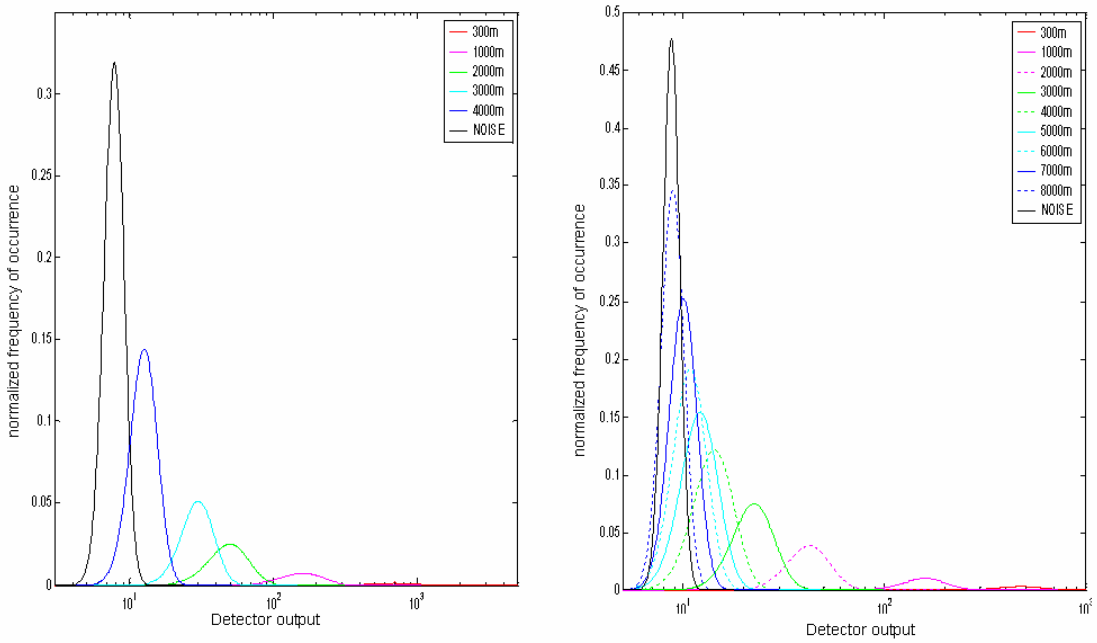

Figure 16: Best fit distributions of the output of matched filter (left) and energy detector (right) based on the interpolated values for g1 and g2 for various ranges given a source level of 143 dB re 1μPa @ 1m.

As shown in **Figure 17,** for a given threshold (x-axis), the probability of false alarm, P(FA), is equal to the area under the noise (leftmost) curve, to the right of threshold. The probability of detection P(D) at a given range is likewise the area under the respective curve to the right of threshold. A useful way to summarize the information contained in the PDF curves is to tabulate P(D) as a function of range and P(FA) as shown in **Table 4** below.

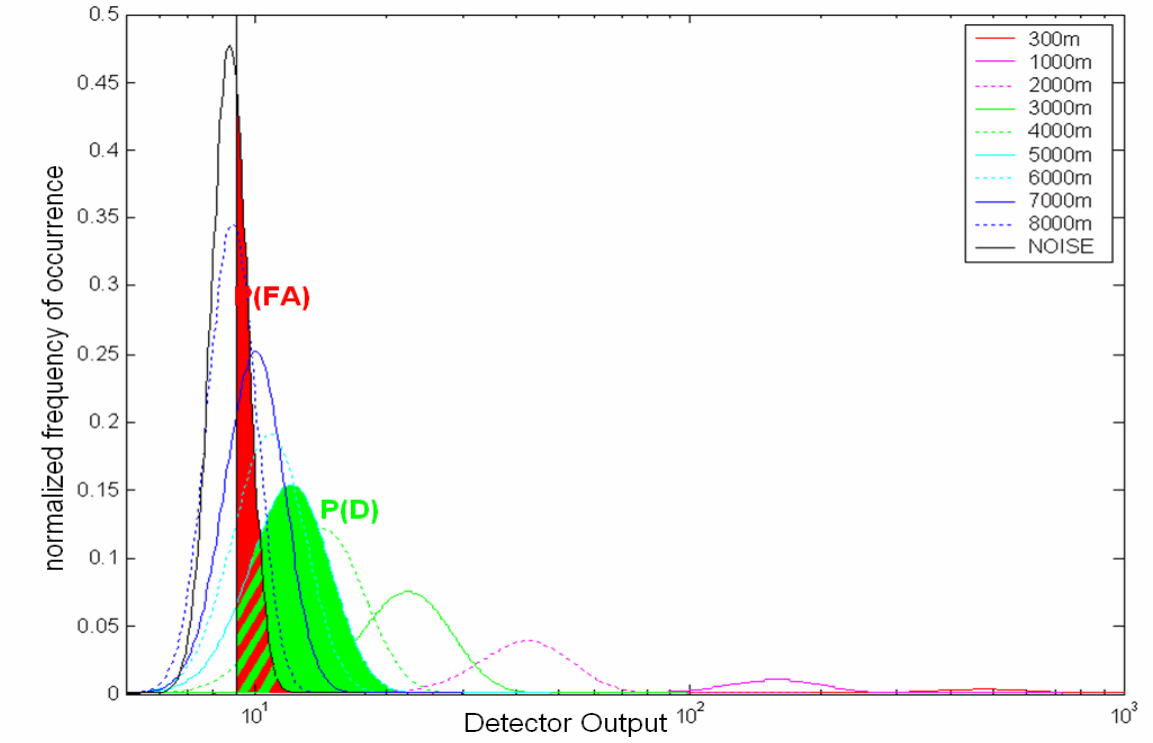

Figure 17: Example of how the PDF curves are used to provide P(D) and P(FA). Integration of a PDF curve from some point T (indicated by the vertical line) to infinity yields the probability (given the conditions that define that curve, such as SL, SNR, range etc…) that an outcome M equal to or greater than T will occur. If T is a detection threshold, then the integration from T to infinity is the probability that M will be "detected."

ENERGY DETECTOR P(D)											
		RANGE(m)									
P(FA)	TRESHOLD	0300	1000	2000	3000	4000	5000	6000	7000	8000	9000
0.1%	10^1.098	100%	100%	100%	99.9%	59.4%					
01%	10^1.055	100%	100%	100%	99.9%	74.5%					
05%	10^1.014	100%	100%	100%	99.9%	85.7%					
10%	10^0.990	100%	100%	100%	100%	90.7%					
20%	10^0.965	100%	100%	100%	100%	94.4%					
MATCHED FILTER P(D)											
		RANGE(m)									
P(FA)	TRESHOLD	0300	1000	2000	3000	4000	5000	6000	7000	8000	9000
0.1%	10^1.07	100%	100%	100%	99.6%	85.2%	64.0%	41.0%	20.3%	2.0%	
01%	10^1.040	100%	100%	100%	99.8%	90.3%	74.1%	54.1%	33.7%	6.2%	
05%	10^1.015	100%	100%	100%	99.9%	93.6%	81.7%	65.5%	47.9%	14.2%	
10%	10^1.001	100%	100%	100%	100%	95.4%	86.0%	72.6%	57.9%	22.6%	

Table 4: Probability of detection P(D) as a function of probability of false alarm P(FA) and range.

B. GENERAL OBSERVATIONS

Here I list a few points which are thought to be relevant to follow-on research even though they were not mentioned in the body of the thesis.

1. Signal Modulation

As illustrated in **Figure 18**, when SNR was high, a pattern of oscillation modulated the outputs of both detectors. The cause of this was not determined. A periodicity of approximately 4 cycles per minute suggested that this modulation was induced by ocean swell. Another possibility is that the oscillation was produced by some rotation of the transducer. This would imply some directionality in the transmission.

The assumption was made that, regardless of its source, this modulation and its effects are a natural consequence of the interaction between an afloat-platform and the marine environment. In other words, no attempt should be made to remove the oscillation in the processing of the data, but rather it should be assimilated into the assessment of performance.

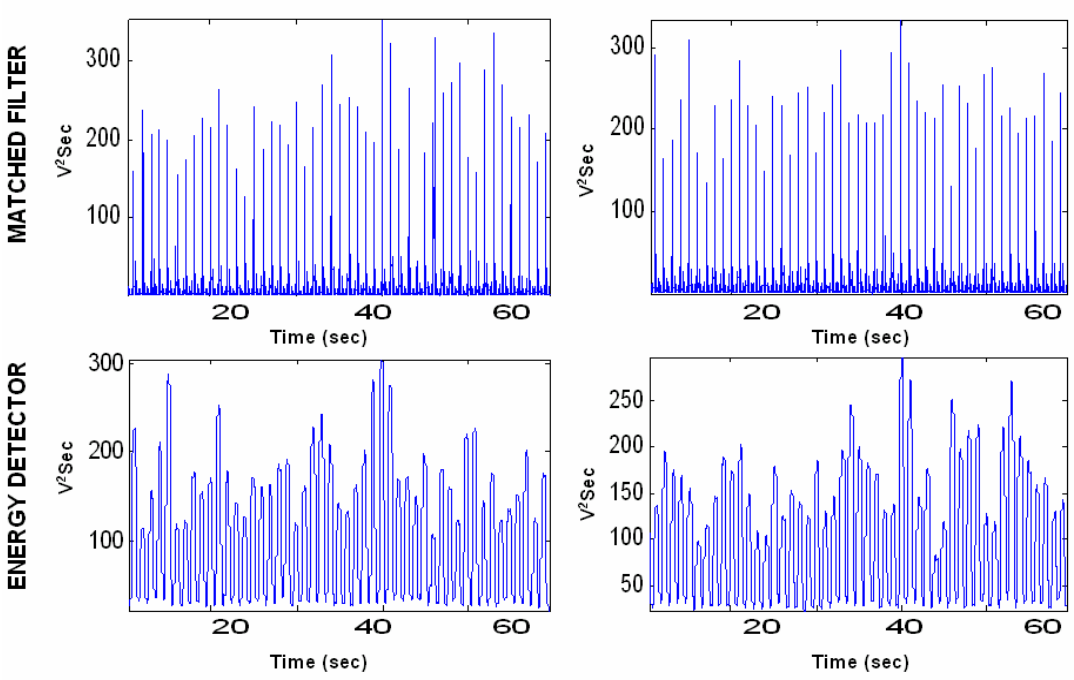

Figure 18: Two sets of detector outputs from different days show a similar "modulating" oscillation with a frequency of approximately four cycles per minute.

2. Discrete Noise Sources

During the course of the experiment, there were a few instances when a tactical bow mounted navy sonar was operated in the vicinity of the SCIUR range. This unplanned circumstance presented the opportunity to observe the effects of a discrete noise source on detector performance. The navy sonar constituted a source of high energy, in band (around 3 kHz) noise. **Figure 19** shows energy detector output and matched filter output corresponding to the same input containing a SONAR ping in the vicinity of 3 kHz.

The unit amplitude box function used in the energy detector acts essentially as the shutter on a camera. The longer the box function is, the higher the exposure on the detector. Since the box is one or more seconds long, the energy detector, like a camera, can be easily overexposed by a high energy source.

The matched filter response to a high energy coherent noise is not as simple. It looks not at pressure squared (power), but at pressure. Because it takes **full** advantage of

the fact that the whale call and the loud noise waveform are not correlated, it is very hard to overexpose (cause a false hit) the matched filter.

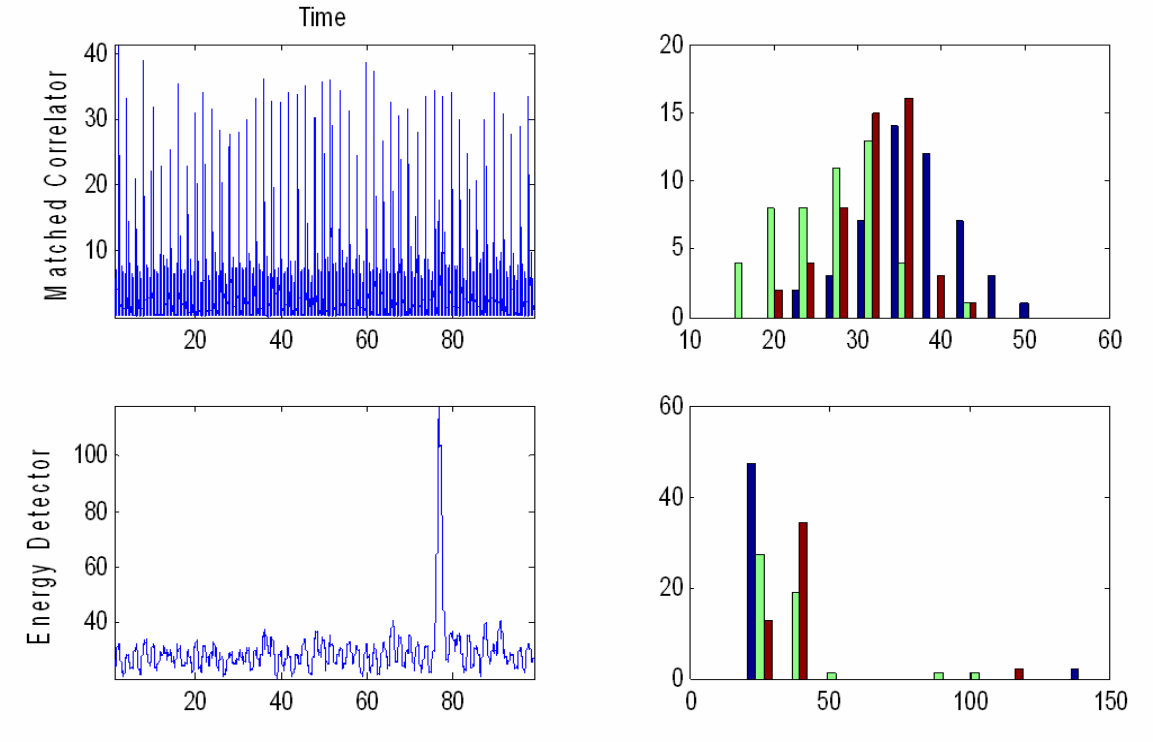

Figure 19: Detector response to 3 kHz navy sonar. The two upper panels are for the matched filter. The two lower panels are for the energy detector. Detector output is shown on the left, and histograms of peak output are on the right (hydrophone-1 output in blue, hydrophone-2 output in green, and hydrophone-3 output in red)

3. Hydrophone-1

Data from hydrophone-1 was found to be unreliable. Most of the time, this hydrophone shows a markedly reduced sensitivity. However, the data from this hydrophone cannot simply be made useful by applying a sensitivity correction since often, it "returns" to the same sensitivity level as the other two hydrophones. **Figure 20** illustrates this erratic behavior of hydrophone-1. Note that the distribution of X for hydrophone 1 is sometimes considerably to the left (reduced sensitivity) and sometimes alongside that of the other two hydrophones. For that reason, no data from hydrophone 1 was used in this thesis. However, it is possible that this data is yet useful, provided that care is taken to ascertain the faulty hydrophone's sensitivity on a case by case basis.

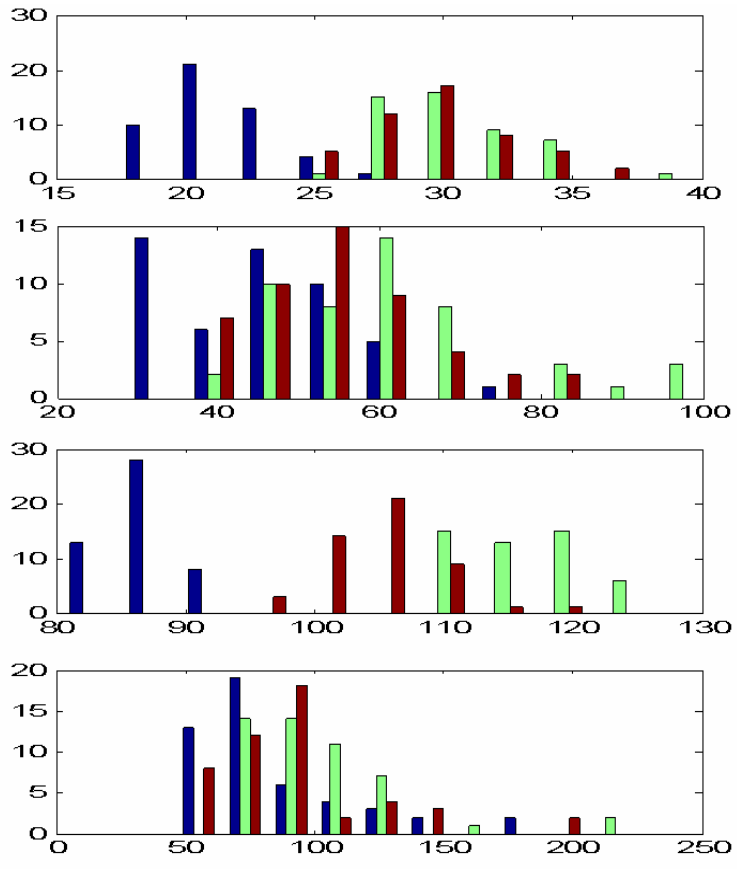

Figure 20: Matched filter detector outputs for the three hydrophones of the San Clemente Island Underwater Range. Four examples are shown. Output peaks are blue for hydrophone-1 green for hydrophone-2, and red for hydrophone-3.

This page intentionally left blank

IV. CONCLUSIONS

The end result of this thesis is summarized by the detector performance curves. A qualitative assessment is made of the effects of range and sea state.

A. PERFORMANCE CURVES

The ultimate objective of this study was to obtain statistical measures of the detector performance. These measures are summarized in the following two figures. **Figure 21** displays the expected performance of the matched filter in terms of the probability of detection as a function of range and as a function of estimated input SNR for a given probability of false alarm. **Figure 22** does the same for the energy detector.

Both detectors' performance is similar in certain respects. Given the source level of 143 dB re 1μPa @ 1 m, a range of 3000 m or less yields a probability of detection near 100% while maintaining a negligible probability of false alarm for both detectors.

For comparison purposes, a maximum detection range can be defined (more or less arbitrarily) as one within which probability of detection is no lower than 90% while probability of false alarm is no greater than 5%. In that case, maximum detection range for the energy detector is approximately 3700 m which corresponds to an input SNR of approximately 0.45. Conversely, the maximum detection range of the matched filter is 4500 m with an input SNR near 0.35 (these ranges are valid given the source level mentioned above). The performance seems comparable, especially when we recall that the matched filter is evaluated using ideal signal conditions (i.e. the source signal is exactly known). However, the energy detector is essentially blind at an input SNR of 0.40 or lower (that is why the curves do not extend beyond this value). On the other hand, the matched filter can be useful with an SNR as low as 0.19 (this, of course would require allowing a greater P(FA) or demanding a lower P(D))

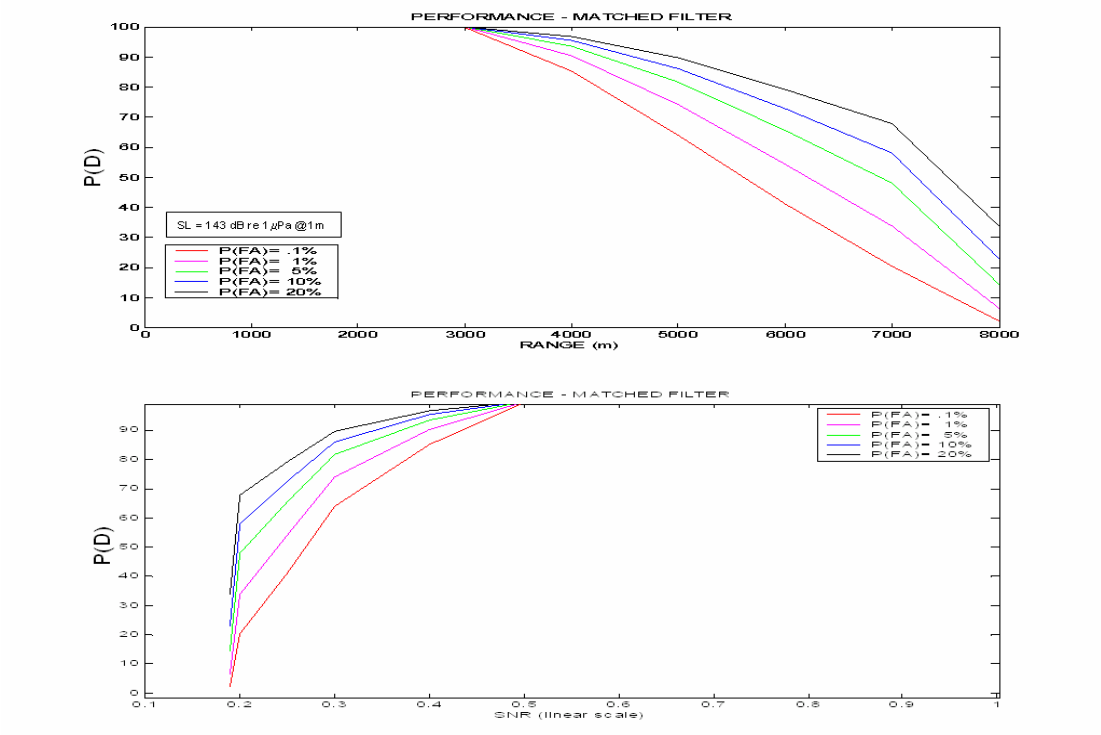

Figure 21: Performance of the matched filter given a SL of 143 dB re 1µPa @1 m.

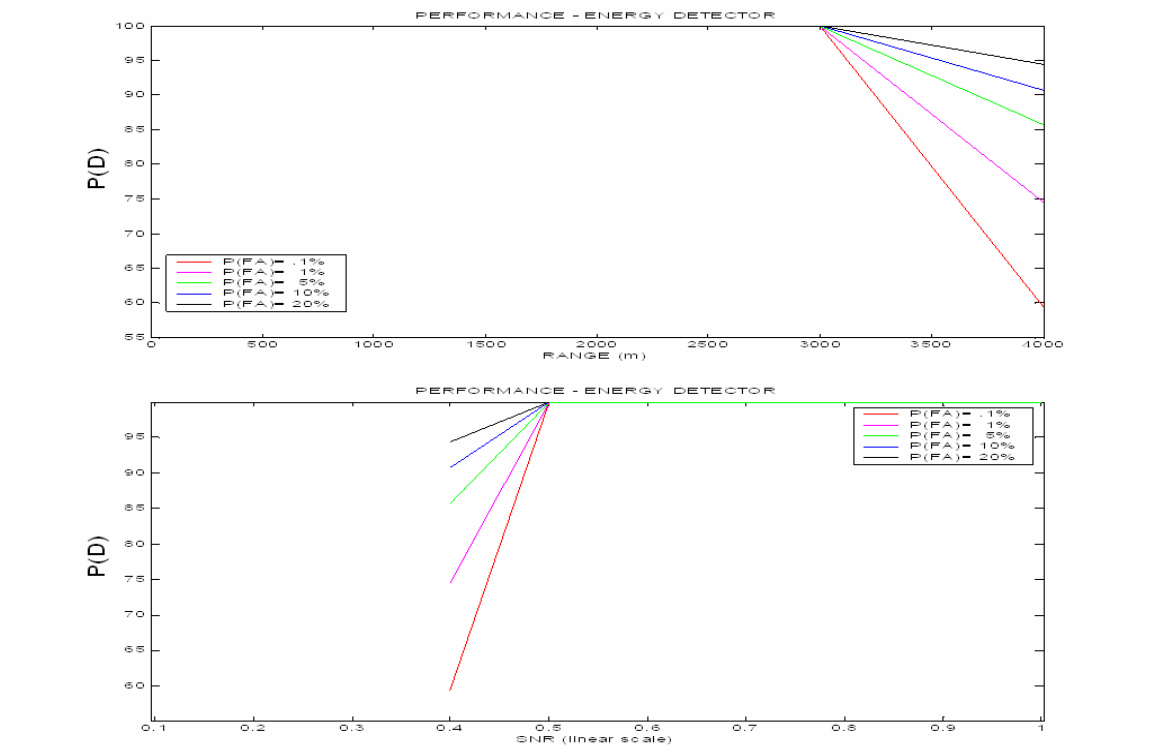

Figure 22: Performance of the energy detector given a SL of 143 dB re 1µPa @1 m.

B. RANGE DEPENDENCE

The comparative performance of the detectors as a function of range is adequately summarized in the results listed in **Table 4**. Both detectors show a very high probability of detection (with minimum probability of false alarm) at short ranges. Probability of detection decreases rapidly to beyond a certain range. Given the source level of 143 dB re 1μPa @ 1 m, this range for the energy detector was usually around three or four thousand meters. For the matched filter, this range was approximately doubled. It must be kept in mind that this performance reflects a matched filter used under ideal circumstances: the reference signal is identical with the "found" signal. When the matched filter was used in non-ideal circumstances (for example, trying to detect **pilo1** using **orca2** as reference), its range dependent performance was equal to or lower than that of the energy detector.

C. SEA STATE DEPENDENCE

There are two ways in which sea state can be expected to affect SNR. First, the surface turbulence may act as a source of background noise (Wenz, 1962). Second, increased surface turbulence will result in increased scattering of sound energy traveling along surface-interacting propagation paths.

An attempt was made to analyze detector performance as a function of surface wave activity (i.e. of homogeneously distributed noise). To this end, average wind speed (taken from two shipboard anemometers) was to be used as a proxy for sea state. However, for this effort to succeed, it would have been necessary to have substantial data gathered while a) range was held constant and b) sea-state changed noticeably.

However, there were only five runs of the experiment and consequently only five sets of constant-range data to compare. Even then, due to the somewhat uncontrollable nature of a ship at sea, range itself was not exactly constant. In the data that was analyzed, no obvious relation between SNR and wind speed or between detector output wind speed was noticed.

Both effects may have in fact been absent during the experiment explaining the absence of correlation between wind and observed acoustics. In the first place, wind generated noise dominates the lower frequencies (30-800 Hz) which are excluded by the detectors' band-pass filters (Kewley, 1989). In the second place, given a downward refracting sound path it is possible that the dominant path for the transmission was non-surface-interacting

APPENDIX A: LOCATION AND WIND DATA

TIME(DD)	RUN	STATION	LAT (deg)	LONG(deg)	DISTANCE (m)	WIND (kts)
ORCA1						
25.7016	1	1	33.0196	118.5256	1180.58	1.67
25.8859	1	7	33.0565	118.4805	6972.64	15.00
25.9109	1	8	33.0634	118.4731	8003.43	13.79
26.1366	2	2	33.0232	118.5168	1964.85	18.34
26.1559	2	3	33.0300	118.5089	3020.08	14.78
26.1953	2	5	33.0432	118.4955	4938.22	17.31
26.6391	3	3	33.0297	118.5091	2981.17	10.00
26.6022	3	5	33.0441	118.4939	5115.28	13.52
26.8578	4	2	33.0252	118.5188	2027.96	11.70
26.8916	4	3	33.0310	118.5109	2985.98	13.46
26.9984	4	6	33.0514	118.4894	6005.20	16.75
27.6891	5	1	33.0162	118.5236	957.85	3.21
27.6559	5	3	33.0299	118.5090	2996.64	1.98
27.6066	5	6	33.0492	118.4887	5861.01	4.54
ORCA2						
25.7047	1	1	33.0200	118.5256	1222.08	1.46
25.7341	1	2	33.0242	118.5155	2119.97	7.96
25.7541	1	3	33.0317	118.5088	3165.66	6.77
25.7703	1	4	33.0373	118.5013	4091.99	8.08
25.7959	1	5	33.0435	118.4937	5077.68	9.24
25.8678	1	6	33.0489	118.4854	6047.28	15.65
25.8891	1	7	33.0564	118.4794	7030.65	15.05
25.9141	1	8	33.0629	118.4718	8045.34	14.77
25.9316	1	9	33.0698	118.4648	9055.76	16.43
25.9503	1	10	33.0753	118.4574	9970.19	17.95
26.1203	2	1	33.0122	118.5292	289.88	14.97
26.1397	2	2	33.0223	118.5161	1926.82	14.37
26.1591	2	3	33.0293	118.5081	3013.26	14.99
26.1984	2	5	33.0423	118.4946	4930.75	15.93
26.7316	3	1	33.0158	118.5218	1049.34	13.42
26.6603	3	2	33.0222	118.5140	2068.39	9.94
26.6422	3	3	33.0294	118.5082	3007.03	10.17
26.6234	3	4	33.0363	118.5013	4011.67	13.59
26.6053	3	5	33.0440	118.4933	5148.92	14.09
26.8609	4	2	33.0247	118.5173	2061.45	13.04
26.8947	4	3	33.0299	118.5095	2974.88	13.95
26.9159	4	4	33.0374	118.5012	4107.18	13.16
26.9778	4	5	33.0429	118.4942	4993.18	16.37
27.0016	4	6	33.0515	118.4912	5907.78	16.04
27.0378	4	7	33.0580	118.4815	7040.71	17.88
27.6922	5	1	33.0166	118.5239	975.74	1.12
27.6591	5	3	33.0297	118.5089	2990.30	2.38
27.6416	5	4	33.0356	118.5025	3876.34	3.44
27.6259	5	5	33.0443	118.4956	5031.86	2.42
27.6097	5	6	33.0485	118.4897	5740.55	2.69
27.5834	5	7	33.0579	118.4808	7073.03	3.81
PILO1						
25.7097	1	1	33.0207	118.5254	1298.26	1.62

25.7397	1	2	33.0248	118.5153	2184.53	8.04
25.7759	1	4	33.0377	118.5009	4154.46	8.24
25.8941	1	7	33.0563	118.4775	7144.28	14.87
25.9191	1	8	33.0628	118.4695	8190.39	16.77
25.9559	1	10	33.0747	118.4550	10074.23	18.06
26.1259	2	1	33.0112	118.5269	377.07	14.18
26.1447	2	2	33.0217	118.5143	2007.10	14.25
26.1641	2	3	33.0287	118.5065	3064.72	14.55
26.2041	2	5	33.0412	118.4927	4959.53	17.38
26.7366	3	1	33.0152	118.5201	1138.23	13.48
26.6472	3	3	33.0287	118.5064	3082.29	12.39
26.8659	4	2	33.0236	118.5149	2119.42	11.57
26.9003	4	3	33.0279	118.5065	3008.41	15.14
26.9834	4	5	33.0415	118.4969	4713.87	18.93
27.0072	4	6	33.0514	118.4945	5707.51	16.50
27.6978	5	1	33.0177	118.5241	1059.90	0.53
27.6641	5	3	33.0299	118.5091	2994.17	2.78
NOISE						
27.2559	5	1	33.0896	118.4460	11854.72	11.09
27.3197	5	2	33.0880	118.4883	9526.05	8.08
27.4584	5	3	33.1188	118.5493	12217.58	7.76
27.4584	5	3	33.1188	118.5493	12217.58	7.76
27.5284	5	4	33.0608	118.4827	7208.25	5.59

LIST OF REFERENCES

Goold, J. C., 1997. "Broadband Spectra of Seismic Survey Air-Gun Emissions, With Reference to Dolphin Auditory Thresholds," Journal of Acoustical Society of America, 103:2177-2184.

Interdisciplinary Center for Bioacoustics and Environmental Research, Pavia, Italy Web Site, Digital Recording of Sperm Whale*, pc_coda.au*, http://www.unipv.it/webcib

Kewley, D. J., 1989. "Low Frequency Wind-Generated Ambient Noise Source Levels," Journal of Acoustical Society of America, 88:1894-1901.

Madsen, P.T., B. Mohl, 1999. "Sperm Whales do not React to Sounds from Detonators," Journal of Acoustical Society of America, 107:668-670.

Ivey, L.E., 1991. "Underwater Electroacoustic Transducers," Naval Research Laboratory, Underwater Sound Reference Detachment, Chapter 2

Newfoundland & Labrador Web Site, Digital Recording of Pilot Whale (pilo2), *Pilot2.wav*, http://www.nfld.com/nfld/other/whales/whales.html

Sjare, B. L., T. G. Smith, 1985. "The Vocal Repertoire of White Whales, *Delphinapterus Leucas*, Summering in Cunningham Inlet, Northwest Territories," Canadian Journal of Zoology, 64: 407-415

Urick R. J., 1983. "Principles of Underwater Sound," McGraw-Hill Book Company, New York, NY.

Vancouver Aquarium, Digital Recording of Transient Orca (orca1), *orca_transien.wav*, http://www.vanaqua.org

Vancouver Aquarium, Digital Recording of Northern Resident Orca (orca2), *orca_northres.wav*, http://www.vanaqua.org

Watkins, W, Digital Recording of Pilot Whale (pilo1), *5721002.wav*, Woods Hole Oceanographic Institute, http://acoustics.whoi.edu

Watkins, W, Digital Recording of Risso's Dolphin, *5902900w.wav*, Woods Hole Oceanographic Institute, http://acoustics.whoi.edu

Wenz, G. M., 1962. "Acoustic Ambient Noise in the Ocean: Spectra and Sources," Journal of Acoustical Society of America, 34:1936-1954.

This page intentionally left blank

INITIAL DISTRIBUTION LIST

1. Defense Technical Information Center
   Ft. Belvoir, VA

2. Dudley Knox Library
   Naval Postgraduate School
   Monterey, CA

3. Dr. Ching-Sang Chiu
   Department of Oceanography
   Naval Postgraduate School
   Monterey, CA

4. Dr. Curtis Collins
   Department of Oceanography
   Naval Postgraduate School
   Monterey, CA

5. Dr. Frank V. Stone
   CNO (N45)
   Crystal Plaza 5
   Arlington, VA

6. Prof. John Hildebrand
   Scripps Institution of Oceanography
   University of California, San Diego
   La Jolla, CA

7. CAPT. Ernie Young, USN (Ret.)
   CNO (N45)
   Crystal Plaza 5
   Arlington, VA

8. Dr. Bob Gisner
   Office of Naval Research
   Arlington, VA

9. Mr. Chris Miller
   Naval Postgraduate School
   Monterey, CA

10. Mr. Anu Kumar
    Naval Postgraduate School
    Monterey, CA

11. LCDR John Daziens
Naval Postgraduate School
Monterey, CA

12. Naval Oceanographic Office Library
Stennis Space Center, MS

13. Dr. Jeff Simmen
Office of Naval Research
Arlington, VA